arXiv:1304.0286v1 [hep-ph] 1 Apr 2013

Prepared for submission to JHEP

The Effect of Composite Resonances on Higgs decay into two photons.

A. E. Cárcamo Hernández, Claudio O. Dib, and Alfonso R. Zerwekh

Universidad Técnica Federico Santa María
and
Centro Científico-Tecnológico de Valparaíso
Casilla 110-V, Valparaíso, Chile

E-mail: antonio.carcamo@usm.cl, claudio.dib@usm.cl,
alfonso.zerwekh@usm.cl

Abstract: In the context of strongly coupled electroweak symmetry breaking, heavy composite particles of different spin and parity may arise and cause observable effects at loop levels. We use an effective chiral lagrangian to describe the interactions amongst these composite resonances and the SM fields. We study the effects of the composite particles on the Higgs decay into two photons and on the oblique T and S parameters. Consistency with the T and S parameters and the newly observed Higgs decay into $\gamma\gamma$ can be found, for axial vector masses in the range 1.7 TeV $\lesssim M_A \lesssim$ 2 TeV and vector masses $\sim 0.8 M_A$, provided a non standard kinetic mixing between the W^3 and B^0 fields is included.

Contents

1 Introduction 1

2 The Effective Chiral Lagrangian with spin-zero and spin-one fields. 3

3 Calculations of the rate $h \to \gamma\gamma$ and the parameters T and S. 9

4 Numerical study of effects on T, S and $h \to \gamma\gamma$. 11

5 Conclusions. 13

A Spontaneously broken $SU(2)_L \times SU(2)_C \times SU(2)_D \times U(1)_Y$ gauge theory 15

B Calculation of the T and S parameters. 20

1 Introduction

The ATLAS and CMS experiments at the CERN Large Hadron Collider (LHC) have found signals consistent with a ~ 126 GeV Higgs boson [1–4]. This discovery offers the possibility to unveil the mechanism of Electroweak Symmetry Breaking (EWSB). Still pending in the LHC studies is to establish the quantum numbers of this particle and to measure its couplings to the standard fermions and gauge bosons. In particular, it is important to determine whether the new observed state comes from a weakly or strongly coupled dynamics. Examples of weakly coupled scenarios of EWSB are the original Higgs sector of the Standard Model, Multi Higgs Models or their Supersymmetric extensions. Alternatively, strong scenarios correspond to composite models such as technicolor theories in their several versions.

The current theory of strong and electroweak interactions, the Standard Model (SM), has proven to be remarkably consistent with all experimental tests, including high precision measurements [5]. However, there are reasons to believe that the SM is only a low energy effective framework of a yet unknown more fundamental theory. One of them is the hierarchy problem, which indicates that new physics should appear at scales not much higher than the EWSB scale (say, around a few TeV) in order to stabilize the Higgs mass at scales much lower than the Planck scale ($\sim 10^{19}$ GeV).

A possible scenario that solves this problem is that of a strongly interacting dynamics without fundamental scalars that becomes non-perturbative somewhere above the EW scale, causing the breakdown of the electroweak symmetry through the formation of condensates in the vacuum [6–11]. In the strongly interacting picture of EWSB, many models have been proposed, which predict the existence of composite particles such as composite scalars [12–40], composite vectors [41–54], composite scalars and vectors [55–71] and composite fermions [72, 73]. These predicted scalar and vector resonances play a very important role in preserving the unitarity of longitudinal gauge boson scattering up to the cutoff $\Lambda \simeq 4\pi v$ [48, 74–80]. One should add that a composite scalar does not have the hierarchy problem since quantum corrections to its mass are saturated at the compositeness scale, which is assumed to be much lower than the Planck scale.

In this work we assume a scenario where there is a strongly interacting sector which possesses a global $SU(2)_L \times SU(2)_R$ symmetry. The strong dynamics spontaneously breaks this global symmetry down to its diagonal $SU(2)_{L+R}$ subgroup. The electroweak gauge group is, in turn, assumed to be contained in the $SU(2)_L \times SU(2)_R$ symmetry, so that the breaking of this symmetry down to the $SU(2)_{L+R}$ subgroup is in fact the realization of electroweak symmetry breaking. Consequently, the interactions among the Standard Model particles and all extra composite resonances can be described by an effective Chiral Lagrangian where the $SU(2)_L \times SU(2)_R$ is non-linearly realized. The explicit $SU(2)_{L+R}$ that remains plays the role of a custodial symmetry of the strong sector, which could be violated by the SM interactions at one loop level. The main sources of breaking of the custodial symmetry come from the hypercharge g' coupling and from the difference between up- and down-type quark Yukawa couplings. The strong dynamics responsible for EWSB, in general gives rise to massive composite vector and axial vector fields (V_μ^a and A_μ^a, respectively) belonging to the triplet representation of the $SU(2)_{L+R}$ custodial group, as well as two massive composite scalars (h and H) and one pseudoscalar (η) all singlets under that group. We will identify the lightest scalar, h, with the state of mass $m_h = 126$ GeV discovered at the LHC. All of these composite resonances are assumed to be lighter than the cutoff $\Lambda \simeq 4\pi v$, so that they explicitly appear as fields in the effective chiral Lagrangian. Composite states of spin 2 and higher are assumed to be heavier than the cutoff, and so are disregarded in this work.

These composite particles are important signatures of the strongly coupled scenarios of EWSB and they could manifest themselves either by direct production or as virtual states in loop corrections. The lack of direct observation at the LHC or any previous collider is expected if their masses are large enough, but their loop effects may still be detectable. In this work we study two processes where loop effects are important: the corrections to the oblique parameters S and T [81–84] and the decay rate $h \to \gamma\gamma$. Specifically, we use the high precision results on S and T to constrain the mass and coupling parameters of the model, and then study the rates of $h \to \gamma\gamma$ which are consistent with the previous constraints and at the same time can explain the recently observed excess of this channel at the LHC.

The organization of the paper is as follows. In Sec. II we introduce our effective Lagrangian that describes the spectrum of the theory. In Sec. III we describe the calculations of our quantities of interest, i.e. the T and S oblique parameters and the rate $h \to \gamma\gamma$, within our model. In Sec. IV we study numerically the constraints on the model parameters, mainly masses and couplings of the extra composite fields, in order to be consistent with the high precision measurements as well as the two-photon signal recently observed in the LHC experiments. Finally in Sec. V we state our conclusions.

2 The Effective Chiral Lagrangian with spin-zero and spin-one fields.

In this work we formulate our strongly coupled sector by means of an effective Chiral Lagrangian that incorporates the heavy composite states by means of local hidden symmetries [85]. As shown in the Appendix A and described in detail in Ref. [48], this Lagrangian is based on the symmetry $G = SU(2)_L \times SU(2)_C \times SU(2)_D \times SU(2)_R$. The $SU(2)_C \times SU(2)_D$ part is a hidden local symmetry whose gauge bosons are linear combinations of the vector and axial vector composites, which we call V^a_μ and A^a_μ respectively, with the SM gauge fields [*cf.* Eq. (A.19) of Appendix A]. The SM gauge group, on the other hand, is contained as a local form of the $SU(2)_L \times SU(2)_R$ global symmetry of the underlying dynamics.

As the symmetry G is spontaneously broken down to the diagonal subgroup $SU(2)_{L+C+D+R}$, it is realized in a non-linear way with the inclusion of three link fields (spin-zero multiplets). These link fields contain two physical scalars h and H, one physical pseudoscalar η, the three would-be Goldstone bosons absorbed as longitudinal modes of the SM gauge fields and the six would-be Goldstone bosons absorbed by the composite triplets V_μ and A_μ.

The starting point is the lowest order chiral Lagrangian for the $SU(2)_L \times SU(2)_R / SU(2)_{L+R}$ Goldstone fields, with the addition of the invariant kinetic terms for the W and B bosons:

$$\mathcal{L}_\chi = \frac{v^2}{4}\left\langle D_\mu U D^\mu U^\dagger \right\rangle - \frac{1}{2g^2}\left\langle W_{\mu\nu} W^{\mu\nu}\right\rangle - \frac{1}{2g'^2}\left\langle B_{\mu\nu} B^{\mu\nu}\right\rangle + \frac{c_{WB}}{4}\left\langle U^\dagger W_{\mu\nu} U B^{\mu\nu}\right\rangle . \quad (2.1)$$

Here $\langle\ \rangle$ denotes the trace over the 2×2 matrices, U is the matrix that contains the SM Goldstone boson fields π^a $(a = 1, 2, 3)$ after the symmetry is spontaneously broken and transforms under $SU(2)_L \times SU(2)_R$ as $U \to g_R U g_L^\dagger$:

$$U = e^{\frac{i}{v}\pi^a \tau^a}, \quad (2.2)$$

being τ^a the Pauli matrices. $D_\mu U$ is the covariant derivative with respect to the SM gauge transformations:

$$D_\mu U = \partial_\mu U - i B_\mu U + i U W_\mu, \quad (2.3)$$

and $W_{\mu\nu}$ and $B_{\mu\nu}$ are the matrix form of the SM tensor fields, respectively,

$$W_{\mu\nu} = \partial_\mu W_\nu - \partial_\nu W_\mu - i\left[W_\mu, W_\nu\right], \quad B_{\mu\nu} = \partial_\mu B_\nu - \partial_\nu B_\mu, \quad (2.4)$$

where $W_\mu = g W^a_\mu\ \tau^a/2$ and $B_\mu = g' B^0_\mu\ \tau^3/2$ are the gauge boson fields in matrix form. Note that we added a kinetic mixing term $W^3 - B^0$, proportional to a (so far arbitrary) coupling c_{WB}.

The vector and axial vector composite fields formed due to the underlying strong dynamics are denoted here as $V_\mu = V^a_\mu \tau^a/\sqrt{2}$ and $A_\mu = A^a_\mu \tau^a/\sqrt{2}$, respectively. They are assumed to be triplets under the unbroken $SU(2)_{L+R}$ symmetry. The parts of the $SU(2)_L \times SU(2)_R$ invariant Lagrangian for the kinetic and mass terms for these fields can be written as:

$$\mathcal{L}_V^{kin} = -\frac{1}{4}\left\langle V_{\mu\nu} V^{\mu\nu}\right\rangle + \frac{1}{2} M_V^2 \left\langle V_\mu V^\mu\right\rangle, \quad \mathcal{L}_A^{kin} = -\frac{1}{4}\left\langle A_{\mu\nu} A^{\mu\nu}\right\rangle + \frac{1}{2} M_A^2 \left\langle A_\mu A^\mu\right\rangle . \quad (2.5)$$

Here the tensor fields $V_{\mu\nu} = \nabla_\mu V_\nu - \nabla_\nu V_\mu$ and $A_{\mu\nu} = \nabla_\mu A_\nu - \nabla_\nu A_\mu$ are written in terms of a covariant derivative in order to include the electroweak gauge symmetry embedded in $SU(2)_L \times SU(2)_R$ [48]:

$$\nabla_\mu V_\nu = \partial_\mu V_\nu + [\Gamma_\mu, V_\nu]\,, \qquad \nabla_\mu A_\nu = \partial_\mu A_\nu + [\Gamma_\mu, A_\nu]\,, \tag{2.6}$$

where the connection Γ_μ satisfies $\Gamma_\mu^\dagger = -\Gamma_\mu$ and is given by:

$$\Gamma_\mu = \frac{1}{2}\left[u^\dagger\left(\partial_\mu - iB_\mu\right)u + u\left(\partial_\mu - iW_\mu\right)u^\dagger\right], \qquad \text{with} \;\; u \equiv \sqrt{U}. \tag{2.7}$$

Assuming that the underlying strong dynamics is invariant under parity and considering the heavy spin-one composite fields as the gauge vectors of a spontaneously broken hidden symmetry, further terms in the Lagrangian appear, which include interactions of these fields with the SM Goldstone bosons and gauge fields. These terms, which are derived in Appendix A, Eq. (A.29), are given by:

$$\begin{aligned}\mathcal{L}_{1V} &= -\frac{f_V}{2\sqrt{2}}\left\langle V^{\mu\nu}\left(uW_{\mu\nu}u^\dagger + u^\dagger B_{\mu\nu}u\right)\right\rangle - \frac{ig_V}{2\sqrt{2}}\left\langle V^{\mu\nu}\left[u_\mu, u_\nu\right]\right\rangle \\ &\quad -\frac{i\kappa f_A}{2\sqrt{2}}\left\langle\left(\partial_\mu u_\nu - \partial_\nu u_\mu + [\Gamma_\mu, u_\nu] - [\Gamma_\nu, u_\mu]\right)[V^\mu, u^\nu]\right\rangle,\end{aligned} \tag{2.8}$$

$$\begin{aligned}\mathcal{L}_{1A} &= \frac{f_A}{2\sqrt{2}}\left\langle\left(\partial_\mu u_\nu - \partial_\nu u_\mu + [\Gamma_\mu, u_\nu] - [\Gamma_\nu, u_\mu]\right)A^{\mu\nu}\right\rangle \\ &\quad -\frac{if_A}{2\sqrt{2}}\left\langle\left(uW_{\mu\nu}u^\dagger + u^\dagger B_{\mu\nu}u\right)[A^\mu, u^\nu]\right\rangle,\end{aligned} \tag{2.9}$$

where $u_\mu = u_\mu^\dagger = iu^\dagger D_\mu U u^\dagger$ is a quantity that transforms covariantly under $SU(2)_{L+R}$. For later convenience we have also redefined the couplings in terms of the dimensionless quantities f_V, g_V and f_A [see Eqs. (A.29) and (A.35) of Appendix A], which depend on the masses of V_μ and A_μ according to:

$$f_V \equiv \frac{1}{g_C} = \sqrt{\frac{1}{1-\kappa}}\,\frac{v}{M_V}, \quad g_V = \frac{1-\kappa^2}{2}f_V, \quad f_A = -\kappa f_V, \tag{2.10}$$

where $\kappa = M_V^2/M_A^2$ [see Eq. (A.35)]. In this way, the interactions of the vector fields V_μ^a with two longitudinal weak bosons are characterized by the coupling g_V, while the interactions of V_μ^a with one longitudinal and one transverse gauge boson are characterized by both g_V and f_V. In turn, the interactions of the axial vector fields A_μ^a with one longitudinal and one transverse gauge boson are characterized by the coupling f_A. Another important feature is the mixings of V_μ^a and of A_μ^a with the Standard Model gauge fields; these mixings are proportional to gf_V and gf_A, respectively.

Now, concerning the interactions of *two* of these spin-one fields with the SM Goldstone bosons and gauge fields, as shown in Appendix A, these are described by the following parts of the Lagrangian:

$$\begin{aligned}\mathcal{L}_{2V} &= -\frac{1-\kappa^2}{8}\left\langle[V_\mu, V_\nu][u^\mu, u^\nu]\right\rangle + \frac{\kappa^2}{8}\left\langle[V_\mu, u_\nu]\left([V^\mu, u^\nu] - [V^\nu, u^\mu]\right)\right\rangle \\ &\quad +\frac{i}{4}\left\langle[V^\mu, V^\nu]\left(uW_{\mu\nu}u^\dagger + u^\dagger B_{\mu\nu}u\right)\right\rangle,\end{aligned} \tag{2.11}$$

$$\mathcal{L}_{2A} = -\frac{1-\kappa^2}{8}\left\langle [A_\mu, A_\nu]\,[u^\mu, u^\nu]\right\rangle + \frac{\kappa^2}{8}\left\langle [A_\mu, u_\nu]\left([A^\mu, u^\nu] - [A^\nu, u^\mu]\right)\right\rangle \\ + \frac{i}{4}\left\langle [A^\mu, A^\nu]\left(uW_{\mu\nu}u^\dagger + u^\dagger B_{\mu\nu}u\right)\right\rangle , \qquad (2.12)$$

$$\mathcal{L}_{1V,1A} = -\frac{i\kappa}{2}\left\langle V_{\mu\nu}\,[A^\mu, u^\nu]\right\rangle - \frac{i\kappa}{2}\left\langle A_{\mu\nu}\,[V^\mu, u^\nu]\right\rangle \\ -\frac{i\kappa}{2}\left\langle \left(\partial_\mu u_\nu - \partial_\nu u_\mu + [\Gamma_\mu, u_\nu] - [\Gamma_\nu, u_\mu]\right)[V^\mu, A^\nu]\right\rangle . \qquad (2.13)$$

In turn, the interactions involving *three* heavy spin-one fields, also derived in Appendix A and included in Eq. (A.29), are described by the terms:

$$\mathcal{L}_{3V} = \frac{ig_C}{2\sqrt{2}}\left\langle V^{\mu\nu}\,[V_\mu, V_\nu]\right\rangle . \qquad (2.14)$$

$$\mathcal{L}_{3A} = -\frac{\kappa g_C}{2\sqrt{2}}\left\langle [A_\mu, A_\nu]\,[A^\mu, u^\nu]\right\rangle , \qquad (2.15)$$

$$\mathcal{L}_{V,2A} = \frac{ig_C}{2\sqrt{2}}\left\langle V_{\mu\nu}\,[A^\mu, A^\nu]\right\rangle + \frac{ig_C}{\sqrt{2}}\left\langle A_{\mu\nu}\,[V^\mu, A^\nu]\right\rangle , \qquad (2.16)$$

$$\mathcal{L}_{A,2V} = -\frac{\kappa g_C}{2\sqrt{2}}\left\langle [V_\mu, V_\nu]\,[A^\mu, u^\nu]\right\rangle - \frac{\kappa g_C}{2\sqrt{2}}\left\langle [V_\mu, u_\nu]\left([V^\mu, A^\nu] - [V^\nu, A^\mu]\right)\right\rangle . \qquad (2.17)$$

The interactions given in (2.14)-(2.17) are controlled by the dimensionless parameter g_C, which is the coupling constant of the hidden local symmetry $SU(2)_C$ and $SU(2)_D$. In particular, $\mathcal{L}_{3V}$ describes the cubic self-interactions of V_μ. Notice that, since $g_C = 1/f_V$ [cf. Eq. (2.10)], these self-interactions are strong when the mixings between the heavy vectors and the SM gauge bosons [cf. Eqs. (2.8, 2.9)] are weak.

Continuing with the expansion given in Eq. (A.29) of Appendix A, the quartic self-interactions of V_μ and of A_μ are proportional to g_C^2, and are described by the terms:

$$\mathcal{L}_{4V} = \frac{g_C^2}{8}\left\langle [V_\mu, V_\nu]\,[V^\mu, V^\nu]\right\rangle , \qquad (2.18)$$

$$\mathcal{L}_{4A} = \frac{g_C^2}{8}\left\langle [A_\mu, A_\nu]\,[A^\mu, A^\nu]\right\rangle . \qquad (2.19)$$

$$\mathcal{L}_{2V2A} = \frac{g_C^2}{4}\left\langle [V_\mu, A_\nu]\left([V^\mu, A^\nu] - [V^\nu, A^\mu]\right)\right\rangle + \frac{g_C^2}{4}\left\langle [V_\mu, V_\nu]\,[A^\mu, A^\nu]\right\rangle . \qquad (2.20)$$

Since V_μ^a and A_μ^a are linear combinations of the gauge bosons of the hidden local symmetry $SU(2)_C \times SU(2)_D$ and of the SM gauge fields [see Eq. (A.19) of Appendix A], the field strength tensors corresponding to the gauge bosons of this hidden local symmetry will include the field strength tensors of V_μ^a and A_μ^a as well as those of the SM gauge bosons [cf. Eqs. (A.21, A.22)]. Because of this reason, additional contact interactions involving the SM gauge fields and Goldstone bosons having couplings depending on f_V, f_A and g_V (see

Eq. 2.10) will automatically emerge from the invariant kinetic terms for the gauge bosons of the $SU(2)_C \times SU(2)_D$ sector. These *contact interactions* are given by:

$$\begin{aligned}\mathcal{L}_{contact} = & -\frac{f_A^2}{8}\left\langle\left(\left(\partial_\mu u_\nu - \partial_\nu u_\mu + [\Gamma_\mu, u_\nu] - [\Gamma_\nu, u_\mu]\right)\right)\left(\left(\partial^\mu u^\nu - \partial^\nu u^\mu + [\Gamma^\mu, u^\nu] - [\Gamma^\nu, u^\mu]\right)\right)\right\rangle \\ & +\frac{g_V^2}{8}\left\langle [u_\mu, u_\nu]\,[u^\mu, u^\nu]\right\rangle - \frac{f_V^2}{8}\left\langle\left(uW_{\mu\nu}u^\dagger + u^\dagger B_{\mu\nu}u\right)\left(uW^{\mu\nu}u^\dagger + u^\dagger B^{\mu\nu}u\right)\right\rangle \\ & -\frac{if_V g_V}{4}\left\langle [u^\mu, u^\nu]\left(uW_{\mu\nu}u^\dagger + u^\dagger B_{\mu\nu}u\right)\right\rangle .\end{aligned} \tag{2.21}$$

These contact terms ensure that the scattering amplitudes involving SM particles have good behaviour at high energies. For example, as shown in Ref. [63], the second term in Eq. (2.21) which contains four derivative terms involving only the SM Goldstone bosons, is crucial for having a consistent description of high energy WW scattering.

In addition to V_μ and A_μ, the underlying strong dynamics after spontaneous symmetry breaking gives rise to two (composite) scalar singlets, h and H, and one pseudoscalar singlet, η. We assume the scalar singlet h to be the $m = 126$GeV boson recently discovered at the LHC, while the other fields are assumed to be heavier. The kinetic and mass terms for these spin zero fields, as well as their interactions with the SM Goldstone bosons and gauge fields, are derived in Eqs. (A.4), (A.31), (A.34) and (A.35) of Appendix A. They are given by:

$$\begin{aligned}\mathcal{L}_h = & \frac{1}{2}\partial_\mu h \partial^\mu h + \frac{m_h^2}{2}h^2 - \frac{g_C^2 v}{2\sqrt{2(1-\kappa)}}h\left\langle V_\mu V^\mu\right\rangle + \frac{g_C^2\left(\frac{1}{\sqrt{\kappa}} - \frac{1}{2\sqrt{1-\kappa}}\right)v}{\sqrt{2}}h\left\langle A_\mu A^\mu\right\rangle \\ & +\frac{\left[2\kappa^{\frac{3}{2}} - (1-\kappa)^{\frac{3}{2}}\right]v}{4\sqrt{2}}h\left\langle u_\mu u^\mu\right\rangle - \frac{g_C\left(\sqrt{1-\kappa} + 2\sqrt{\kappa}\right)v}{2}h\left\langle A_\mu u^\mu\right\rangle ,\end{aligned} \tag{2.22}$$

$$\begin{aligned}\mathcal{L}_H = & \frac{1}{2}\partial_\mu H \partial^\mu H + \frac{m_H^2}{2}H^2 + \frac{g_C^2 v}{2\sqrt{2(1-\kappa)}}H\left\langle V_\mu V^\mu\right\rangle + \frac{g_C^2\left(\frac{1}{\sqrt{\kappa}} + \frac{1}{2\sqrt{1-\kappa}}\right)v}{\sqrt{2}}H\left\langle A_\mu A^\mu\right\rangle \\ & +\frac{\left[2\kappa^{\frac{3}{2}} + (1-\kappa)^{\frac{3}{2}}\right]v}{4\sqrt{2}}H\left\langle u_\mu u^\mu\right\rangle + \frac{g_C\left(\sqrt{1-\kappa} - 2\sqrt{\kappa}\right)v}{2}H\left\langle A_\mu u^\mu\right\rangle ,\end{aligned} \tag{2.23}$$

$$\mathcal{L}_\eta = \frac{1}{2}\partial_\mu \eta \partial^\mu \eta + \frac{m_\eta^2}{2}\eta^2 + \frac{g_C^2 v}{\sqrt{1-\kappa}}\left\langle V_\mu A^\mu\right\rangle\eta + \frac{g_C\sqrt{1-\kappa}v}{\sqrt{2}}\left\langle V_\mu u^\mu\right\rangle\eta . \tag{2.24}$$

In turn, the interaction terms that include two of these spin-zero fields coupled to the SM Goldstone bosons or gauge fields, or to the composite V_μ and A_μ fields, are also derived in Appendix A, Eqs. (A.31), (A.34) and (A.35). They are given by:

$$\begin{aligned}\mathcal{L}_{2h} = & \frac{g_C^2}{16}h^2\left\langle V_\mu V^\mu\right\rangle + \frac{5g_C^2}{8}h^2\left\langle A_\mu A^\mu\right\rangle + \frac{1}{32}\left[(1-\kappa)^2 + 4\kappa^2\right]h^2\left\langle u_\mu u^\mu\right\rangle \\ & +\frac{g_C(1-5\kappa)}{8\sqrt{2}}h^2\left\langle A_\mu u^\mu\right\rangle ,\end{aligned} \tag{2.25}$$

$$\begin{aligned}\mathcal{L}_{2H} =& \frac{g_C^2}{16}H^2\left\langle V_\mu V^\mu\right\rangle + \frac{5g_C^2}{8}H^2\left\langle A_\mu A^\mu\right\rangle + \frac{1}{32}\left[(1-\kappa)^2+4\kappa^2\right]H^2\left\langle u_\mu u^\mu\right\rangle \\ &+\frac{g_C\left(1-5\kappa\right)}{8\sqrt{2}}H^2\left\langle A_\mu u^\mu\right\rangle ,\end{aligned} \tag{2.26}$$

$$\begin{aligned}\mathcal{L}_{2\eta} =& \frac{g_C^2}{8}\eta^2\left\langle V_\mu V^\mu\right\rangle + \frac{g_C^2}{8}\eta^2\left\langle A_\mu A^\mu\right\rangle + \frac{(1-\kappa)^2}{16}\eta^2\left\langle u_\mu u^\mu\right\rangle \\ &+\frac{g_C\left(1-\kappa\right)}{4\sqrt{2}}\eta^2\left\langle A_\mu u^\mu\right\rangle ,\end{aligned} \tag{2.27}$$

$$\begin{aligned}\mathcal{L}_{hH} =& -\frac{g_C^2}{8}hH\left\langle V_\mu V^\mu\right\rangle + \frac{3g_C^2}{8}hH\left\langle A_\mu A^\mu\right\rangle + \frac{4\kappa^2-(1-\kappa)^2}{16}hH\left\langle u_\mu u^\mu\right\rangle \\ &-\frac{g_C\left(1+3\kappa\right)}{4\sqrt{2}}hH\left\langle A_\mu u^\mu\right\rangle ,\end{aligned} \tag{2.28}$$

$$\mathcal{L}_{h\eta} = -\frac{g_C^2}{2\sqrt{2}}\left\langle V_\mu A^\mu\right\rangle h\eta - \frac{(1-\kappa)\,g_C}{4}\left\langle V_\mu u^\mu\right\rangle h\eta, \tag{2.29}$$

$$\mathcal{L}_{H\eta} = \frac{g_C^2}{2\sqrt{2}}\left\langle V_\mu A^\mu\right\rangle H\eta + \frac{(1-\kappa)\,g_C}{4}\left\langle V_\mu u^\mu\right\rangle H\eta. \tag{2.30}$$

Finally, we also consider the mass terms for the SM quarks as well as interactions between the light Higgs field h and the SM fermions as originating from Yukawa-type terms of the form:

$$\mathcal{L}_h^Y = -\frac{v}{\sqrt{2}}\sum_{i,j}\left(\bar{u}_L^{(i)} d_L^{(i)}\right) U \left(1+a_{hff}\,\frac{h}{v}\right)\begin{pmatrix}\lambda_{ij}^u\, u_R^{(j)} \\ \lambda_{ij}^d\, d_R^{(j)}\end{pmatrix} + h.c., \tag{2.31}$$

where λ_{ij}^u and λ_{ij}^d are the *up* and *down* type quarks Yukawa couplings, respectively. Here a_{hff} parametrizes in our model a deviation factor from the SM Higgs-fermion coupling (in the SM this factor is unity). In order to cancel the growth of the $W_L W_L \to \bar{f}f$ scattering amplitude at high energies (where f represents Standard fermions), a_{hff} should satisfy [16, 63]:

$$a_{hff} = \frac{1}{a_{hWW}} = \frac{2\sqrt{2}}{2\kappa^{\frac{3}{2}} - (1-\kappa)^{\frac{3}{2}}}, \tag{2.32}$$

where a_{hWW}, in obvious notation, represents an extra numerical factor in the coupling hWW (also of value unity in the Standard Model).

Since the vectors V_μ as well as the scalars h and H contribute to the elastic WW scattering amplitude, a good asymptotic behaviour of the latter amplitude at high energies will yield a relation between the a_{hWW}, a_{HWW} and g_V parameters. Because of the extra contributions of the heavy scalar H and of the heavy vectors V_μ in our model with respect to the SM case, a_{hWW} will turn out to be different than unity. Then, the unitarity constraint in both the elastic WW scattering as well as in $WW \to \bar{f}f$ scattering implies that a_{hff} must also differ from unity, in the way described by Eq. (2.32).

Summarizing, in the framework of strongly interacting dynamics for EWSB, the low energy interactions among the composite spin-zero fields, the composite triplets of spin-one fields, the SM gauge bosons, SM Goldstone bosons and the SM fermions can be described by the following $SU(2)_L \times SU(2)_R / SU(2)_{L+R}$ chiral Lagrangian:

$$\begin{aligned}\mathcal{L}_{eff} = & \mathcal{L}_{\chi} + \mathcal{L}_{V}^{kin} + \mathcal{L}_{A}^{kin} + \mathcal{L}_{1V} + \mathcal{L}_{1A} + \mathcal{L}_{2V} + \mathcal{L}_{2A} + \mathcal{L}_{1V,1A} + \mathcal{L}_{3V} + \mathcal{L}_{3A} \\ & + \mathcal{L}_{V,2A} + \mathcal{L}_{A,2V} + \mathcal{L}_{4V} + \mathcal{L}_{4A} + \mathcal{L}_{2V2A} + \mathcal{L}_{contact} + \mathcal{L}_{h} + \mathcal{L}_{H} + \mathcal{L}_{\eta} \\ & + \mathcal{L}_{2h} + \mathcal{L}_{2H} + \mathcal{L}_{2\eta} + \mathcal{L}_{hH} + \mathcal{L}_{h\eta} + \mathcal{L}_{H\eta} + \mathcal{L}_{h}^{Y} . \end{aligned} \tag{2.33}$$

The above Lagrangian, excluding the Yukawa interaction as well as the modified kinetic $W^3 - B^0$ mixing (described by the coupling c_{WB}), can be obtained from a gauge theory based on $SU(2)_L \times SU(2)_C \times SU(2)_D \times U(1)_Y$ spontaneously broken by three Higgs doublets as shown in Appendix A. This construction guarantees that the scattering amplitudes will be well behaved at high energies, keeping under control the unitarity of the effective theory up to the scale of spontaneous symmetry breaking. Our effective theory is based on the following assumptions:

1. The Lagrangian responsible for EWSB has an underlying strong dynamics with a global $SU(2)_L \times SU(2)_R$ symmetry which is spontaneously broken by the strong dynamics down to the $SU(2)_{L+R}$ custodial group. The SM electroweak gauge symmetry $SU(2)_L \times U(1)_Y$ is assumed to be embedded as a local part of the $SU(2)_L \times SU(2)_R$ symmetry. Thus the spontaneous breaking of $SU(2)_L \times SU(2)_R$ also leads to the breaking of the electroweak gauge symmetry down to $U(1)_{em}$.

2. The strong dynamics produces composite heavy vector fields V_μ^a and axial vector fields A_μ^a, triplets under the custodial $SU(2)_{L+R}$, as well as a composite scalar singlet h with mass $m_h = 126$ GeV, a heavier scalar singlet H, and a heavier pseudoscalar singlet η. These fields are assumed to be the only composites lighter than the symmetry breaking cutoff $\Lambda \simeq 4\pi v$.

3. The heavy fields V_μ^a and A_μ^a couple to SM fermions only through their kinetic mixings with the SM Gauge bosons.

4. The lighter scalar singlet h interacts with the fermions only via (proto)-Yukawa couplings. The heavy scalar H and pseudoscalar η are fermiofobic.

Our Lagrangian has in total five extra free parameters: the modified kinetic $W^3 - B^0$ mixing coupling c_{WB}, the heavy vector and heavy axial vector masses M_V and M_A, and the heavy scalar and heavy pseudoscalar masses m_H and m_η. However, from the expressions in Appendix B we can see that the oblique T and S parameters have a low sensitivity to the masses of H and η. Therefore, taking into account the experimental bound 600 GeV $\lesssim m_H, m_\eta \lesssim 1$ TeV for heavy spin-0 particles, without much loss of generality we can fix $m_H = m_\eta = 1$ TeV. We are then left with three free parameters: c_{WB}, M_V and M_A. In what follows, we will constrain these parameters according to the current status of high precision measurements and study the deviation from the SM predictions on $h \to \gamma\gamma$.

3 Calculations of the rate $h \to \gamma\gamma$ and the parameters T and S.

In the Standard Model, the $h \to \gamma\gamma$ decay is dominated by W loop diagrams which can interfere destructively with the subdominant top quark loop. In our strongly coupled model, the $h \to \gamma\gamma$ decay receives extra contributions from loops with charged V_μ and A_μ, as shown in Figure 1. The explicit form for the $h \to \gamma\gamma$ decay width is given by:

$$\Gamma\left(h \to \gamma\gamma\right) = \frac{\alpha_{em}^2 m_h^3}{256\pi^3 v^2} \left| \sum_f a_{hff} N_c Q_f^2 F_{1/2}\left(\beta_f\right) + a_{hWW} F_1\left(\beta_W\right) \right. \\ \left. + a_{hVV} F_1\left(\beta_V\right) + a_{hAA} F_1\left(\beta_A\right) \right|^2 , \tag{3.1}$$

where a_{hff} and a_{hWW} are given in Eqs. (2.32), while

$$a_{hVV} = -\frac{(1-\kappa)^{\frac{1}{2}}}{2\sqrt{2}}, \quad a_{hAA} = \kappa\left(1 - 2\sqrt{\frac{1-\kappa}{\kappa}}\right) a_{hVV}. \tag{3.2}$$

Here β_i are the mass ratios $\beta_i = m_h^2/4M_i^2$, with $M_i = m_f, M_W, M_V$ and M_A, respectively, α_{em} is the fine structure constant, N_C is the color factor ($N_C = 1$ for leptons, $N_C = 3$ for quarks), and Q_f is the electric charge of the fermion in the loop. We should recall that $\kappa = M_V^2/M_A^2$ and $M_V = g_C v/\sqrt{1-\kappa}$, as shown in Eq. (A.35). For the contribution from the fermion loops we will only keep the dominant term, which is the one involving the top quark.

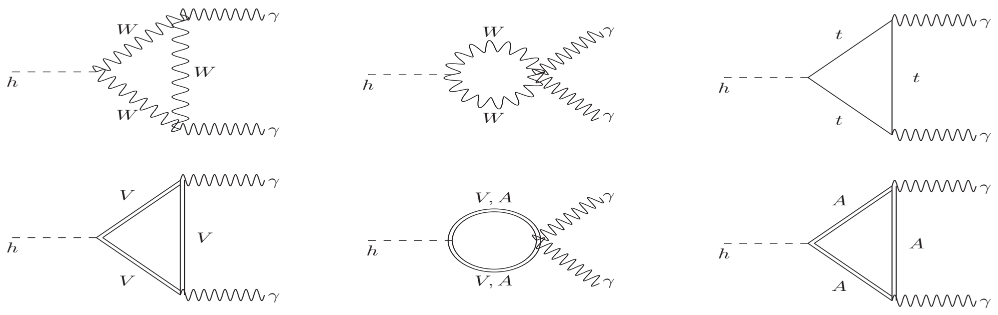

Figure 1. One loop Feynman diagrams in the Unitary Gauge contributing to the $h \to \gamma\gamma$ decay.

The dimensionless loop factors $F_{1/2}\left(\beta\right)$ and $F_1\left(\beta\right)$ (for particles of spin 1/2 and 1, respectively) are [86–93]:

$$F_{1/2}\left(\beta\right) = 2\left[\beta + \left(\beta - 1\right) f\left(\beta\right)\right]\beta^{-2}, \quad F_1\left(\beta\right) = -\left[2\beta^2 + 3\beta + 3\left(2\beta - 1\right) f\left(\beta\right)\right]\beta^{-2}, \tag{3.3}$$

with

$$f(\beta) = \begin{cases} \arcsin^2 \sqrt{\beta}, & \textit{for} \;\; \beta \leq 1 \\ -\frac{1}{4}\left[\ln\left(\frac{1+\sqrt{1-\beta^{-1}}}{1-\sqrt{1-\beta^{-1}}}\right) - i\pi\right]^2, & \textit{for} \;\; \beta > 1. \end{cases} \tag{3.4}$$

From the previous expressions it follows that the heavy vector contribution to the $h \to \gamma\gamma$ decay strongly dominates over the axial vector contribution when $M_V \ll M_A$, since in this case we have $a_{hVV} \gg a_{hAA}$.

In this work we want to determine the range of the heavy vector masses which is consistent with the events in the $h \to \gamma\gamma$ decay recently observed at the LHC. To this end, we will introduce the ratio $R_{\gamma\gamma}$, which measures the $\gamma\gamma$ signal produced in our model relative to the signal within the SM:

$$R_{\gamma\gamma} = \frac{\sigma\left(pp \to h\right)\Gamma\left(h \to \gamma\gamma\right)}{\sigma\left(pp \to h\right)_{SM}\Gamma\left(h \to \gamma\gamma\right)_{SM}} \simeq a_{htt}^2 \frac{\Gamma\left(h \to \gamma\gamma\right)}{\Gamma\left(h \to \gamma\gamma\right)_{SM}}. \tag{3.5}$$

This normalization of the branching ratio of $h \to \gamma\gamma$ to the SM prediction was also done in Ref.[94]. Here we have taken into account the fact that in our model the single higgs production is dominated by gluon fusion as in the Standard Model.

The inclusion of the extra composite particles also modifies the oblique corrections of the SM, which have been obtained in high precision experiments. Consequently, the validity of our model depends on the condition that the extra particles do not contradict those experimental results. These oblique corrections are parametrized in terms of the two well known quantities T and S. The T parameter is defined as [81–84]:

$$T = \frac{\Pi_{33}\left(0\right) - \Pi_{11}\left(0\right)}{M_W^2 \; \alpha_{em}\left(m_Z\right)}. \tag{3.6}$$

where $\Pi_{11}\left(0\right)$ and $\Pi_{33}\left(0\right)$ are the vacuum polarization amplitudes for loop diagrams having gauge bosons W_μ^1, W_μ^1 and W_μ^3, W_μ^3 in the external lines, respectively. These vacuum polarization amplitudes are evaluated at $q^2 = 0$, where q the external momentum. The one-loop diagrams that give contributions to the T parameter should include the hypercharge gauge boson B_μ^0 since the g' coupling is one of the sources of the breaking of the custodial symmetry. The other source of custodial symmetry breaking comes from the difference between up and down type quark Yukawa couplings.

Now, considering the S parameter, it is defined as [81–84]:

$$S = \frac{4\sin^2\theta_W}{\alpha_{em}\left(m_Z\right)} \frac{g}{g'} \frac{d\Pi_{30}\left(q^2\right)}{dq^2}\bigg|_{q^2=0}, \tag{3.7}$$

where $\Pi_{30}\left(q^2\right)$ is the vacuum polarization amplitude for a loop diagram having W_μ^3 and B_μ in the external lines.

The corresponding Feynman diagrams and details of the lengthy calculation of T and S that includes the extra particles in the loops are included in Appendix B.

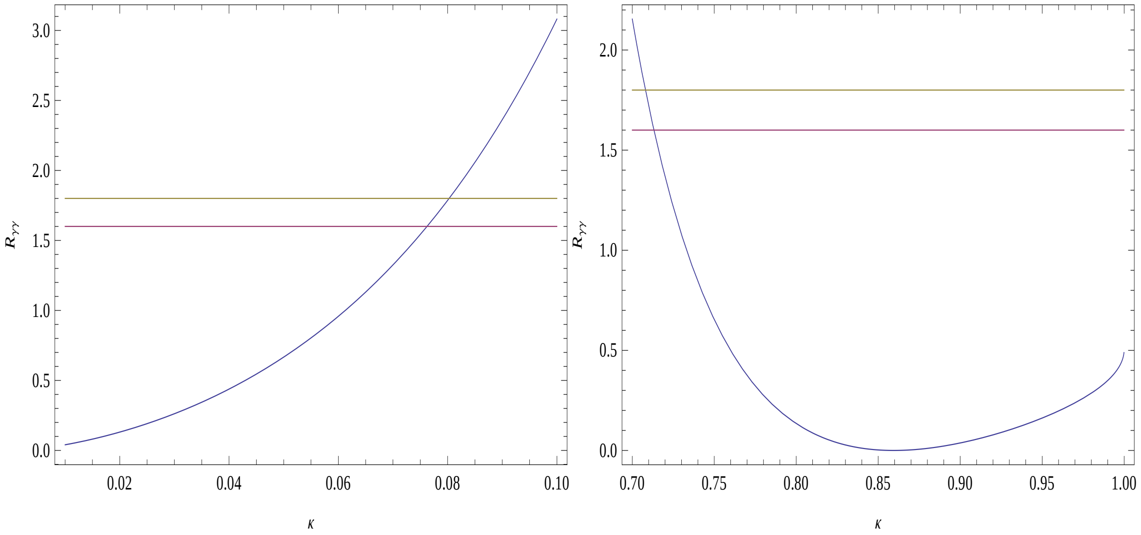

(2.a) (2.b)

Figure 2. The ratio $R_{\gamma\gamma}$ as a function of κ for $g_C v = 0.8$ TeV. The horizontal lines are the $R_{\gamma\gamma}$ experimental values given by CMS and ATLAS, which are equal to 1.6 ± 0.4 and $1.8 \pm^{0.460}_{0.419}$, respectively [95–98].

4 Numerical study of effects on T, S and $h \to \gamma\gamma$.

Let us first study the κ dependence ($\kappa = M_V^2/M_A^2$) of the two-photon signal, given in terms of the ratio $R_{\gamma\gamma}$ of Eq. (3.5), trying to find values in the range $R_{\gamma\gamma} \sim 1 - 2$. In Fig. 2 we show $R_{\gamma\gamma}$ as a function of κ, for a fixed value $g_C v = 0.8$ TeV. This value for $g_C v$ was chosen in order to fulfill the condition $\frac{g_C^2}{4\pi} \lesssim 1$, which implies $g_C v \lesssim 0.9$ TeV. In any case, we checked that our signal $R_{\gamma\gamma}$ stays almost at the same value when the scale $g_C v$ is varied from 0.8 TeV to 1 TeV. This is so because the loop function $F_1(\beta)$ [see Eq. (3.3)] has a very low sensitivity to β in the corresponding range.

As shown in Fig. 2, $R_{\gamma\gamma} \approx 1.7$ is obtained for $\kappa \approx 0.078$ and 0.71, which means a ratio M_V/M_A close to 0.28 or 0.84, respectively, in order to explain the excess of events in the $h \to \gamma\gamma$ decay recently observed at the LHC. In a looser way, in order to get $1 \lesssim R_{\gamma\gamma} \lesssim 2$ we find that κ has to be in the range $0.061 \leq \kappa \leq 0.084$ or $0.70 \leq \kappa \leq 0.73$. The range $0.1 < \kappa < 0.7$ is excluded because in this range $\frac{a_{htt}^2}{4\pi} >> 1$ and $R_{\gamma\gamma}$ gets unacceptably large values. In that range, the one-loop computation of $R_{\gamma\gamma}$ becomes unreliable.

Let us now analyze the constraints imposed on the parameters by the values of T and S given by the experimental high precision tests of electroweak interactions. As shown in Appendix B, in general the expressions for T and S exhibit quartic, quadratic and logarithmic dependence on the cutoff $\Lambda \sim 3$ TeV. However, the contributions coming from loops containing the h, H and η scalars are independent of the cutoff, except for a logarithmic dependence in the case of diagrams containing a scalar and a hypercharge gauge boson, and at most a quadratic dependence in the contact scalar loop contributions to the S parameter. As a consequence, T and S happen to have a rather mild sensitivity to the masses of H and η, and so we will restrict our study to a scenario where H and η are degenerate in mass at a value of 1 TeV. In contrast, most of the other diagrams, i.e. those containing SM bosons and/or the composite spin-1 fields V_μ or A_μ, have quartic and quadratic dependence on the cutoff, and as a consequence they are very sensitive to the masses M_V and M_A.

The definition of the T and S parameters and their calculation within our model are given in Appendix B [see Eqs. (B.1) and (B.30)]. We can separate the contributions to T and S as $T = T_{SM} + \Delta T$ and $S = S_{SM} + \Delta S$, where

$$T_{SM} = -\frac{3}{16\pi \cos^2\theta_W}, \qquad S_{SM} = \frac{1}{12\pi}\ln\left(\frac{m_h^2}{m_W^2}\right) \tag{4.1}$$

are the contributions within the SM, while ΔT and ΔS contain all the contributions involving the extra particles.

Then, the experimental results on T and S impose the restriction that ΔT and ΔS must lie inside a region in the $\Delta S - \Delta T$ plane. Explicitly, the experimentally allowed region at the 95%CL in the $\Delta S - \Delta T$ plane is the ellipse shown in Figs. 3.

In order to have ΔT inside that region, we find that M_A should have a value in the range 1.76 TeV−2.15 TeV and $M_V \simeq 0.84 M_A$, in order to satisfy these constraints, and at the same time yield a $h \to \gamma\gamma$ signal near the recent experimental observations at the LHC. For numerical purposes, we then proceed to select a few representative discrete values of the axial vector mass M_A, namely 1.76 TeV, 1.9 TeV and 2.15 TeV, and then compute the resulting T and S parameters.

Accordingly, for the three chosen cases, namely $M_A = 1.76$ TeV, 1.9 TeV and 2.15 TeV, we find that the corresponding values of M_V must be 1.48 TeV, 1.6 TeV and 1.81 TeV in order to have an excess of events in the $h \to \gamma\gamma$ decay $R_{\gamma\gamma} \simeq 1.7$. Note that we have discarded the case $M_V/M_A \sim 0.28$, which also gives $R_{\gamma\gamma} \simeq 1.7$ [see Fig. 2.a], since in that case ΔT falls outside the experimental bounds.

Now, continuing with the analysis of the constraints in the $\Delta T - \Delta S$ plane, we also find that, in order to fulfill the constraint on ΔS as well, an additional condition must be met: for the aforementioned range of values of M_V and M_A, the S parameter turns out to be unacceptably large, unless a modified $W^3 - B^0$ mixing is added. Here we introduce this mixing in terms of a coupling c_{WB} [see Eq. (2.1)]. While ΔT does not depend much on this coupling, ΔS does depend on it, because this coupling enters in the quadratically divergent loop diagrams involving the $\pi^1\pi^1W^3B^0$ and $\pi^2\pi^2W^3B^0$ contact interactions (where π^i are the SM Goldstone bosons), as well as in the $W^3 - B^0$ tree level mixing diagram.

As it is shown in Figs. 3, we find that the coupling c_{WB} should be in the ranges $0.233 \le c_{WB} \le 0.235$, $0.186 \le c_{WB} \le 0.189$ and $0.132 \le c_{WB} \le 0.133$ for the cases M_A =1.76 TeV, 1.9 TeV and 2.15 TeV, respectively.

In Figs. 3.a, 3.b and 3.c we show the allowed regions for the ΔT and ΔS parameters, for three different sets of values of M_V and M_A. The ellipses denote the experimentally allowed region at 95% C.L., while the horizontal line shows the values of ΔT and ΔS in the model, as the mixing parameter c_{WB} is varied over the specified range in each case. As shown, ΔT does not depend on c_{WB} (i.e. the line is horizontal), while ΔS does. Moreover, the ranges for c_{WB} clearly exclude the case $c_{WB} = 0$, as ΔS would fall outside the allowed region (the point would be further to the left of the corresponding ellipse).

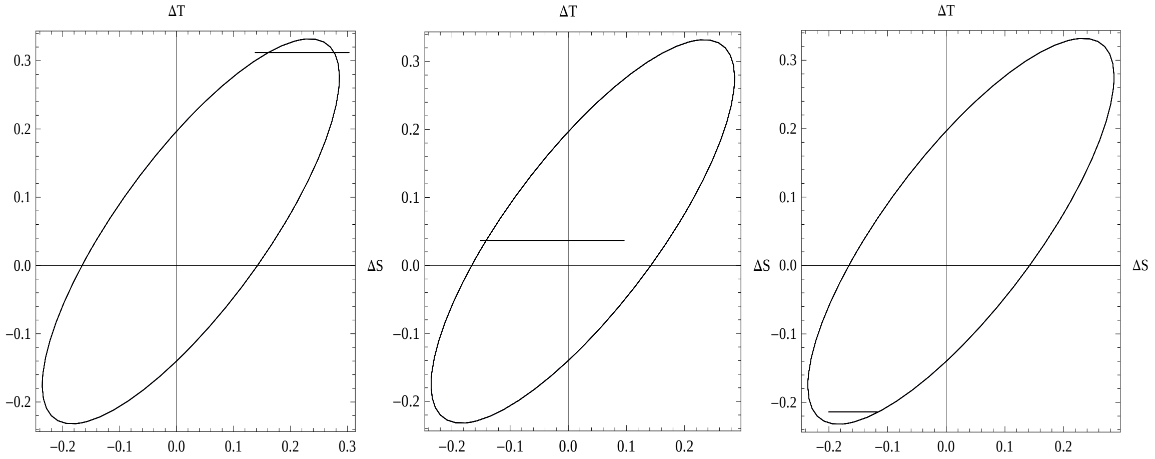

$M_A = 1.76$ TeV, $M_V = 1.48$ TeV
(3.a)

$M_A = 1.9$ TeV, $M_V = 1.6$ TeV
(3.b)

$M_A = 2.15$ TeV, $M_V = 1.81$ TeV
(3.c)

Figure 3. The $\Delta S - \Delta T$ plane in our model with composite scalars and vector fields. The ellipses denote the experimentally allowed region at 95%CL taken from [99]. The origin $\Delta S = \Delta T = 0$ corresponds to the Standard Model value, with $m_h = 125.7$ GeV and $m_t = 176$ GeV. Figures a, b and c correspond to three different sets of values for the masses M_V and M_A, as indicated. The horizontal line shows the values of ΔS and ΔT in the model, as the mixing parameter c_{WB} varies over the ranges $0.233 \leq c_{WB} \leq 0.235$ (Fig. 3.a), $0.186 \leq c_{WB} \leq 0.189$ (Fig. 3.b), and $0.132 \leq c_{WB} \leq 0.133$ (Fig. 3.c).

As a final remark, we should notice that our results differ from those of Ref. [100], where the consistency with EWPT requires heavy vector masses larger than about 1.5 TeV. However, our model is different from the model of Ref. [100] in the sense that they use a tensor formulation instead of a vector formulation to describe the heavy spin-one fields, their spectrum does not include a pseudoscalar and, more important, the interactions involving more than one heavy spin-one field are not considered, so that vertices like hVV and hAA are absent. This implies that the heavy spin-one particles do not play a role in the $h \to \gamma\gamma$ decay. However, that model does consider an interaction between the scalar, the SM gauge bosons and the axial vector involving a covariant derivative of the scalar field. We do not consider this interaction in the present work and we defer for a future study the inclusion of that interaction and the study of its effects in EWPT and $h \to \gamma\gamma$ decay.

5 Conclusions.

We considered a framework of electroweak symmetry breaking without fundamental scalars, based on an underlying dynamics that becomes strong at a scale which we assume $\Lambda \sim 3$ TeV. In general, below this scale there could be composite fields, bound by the strong dynamics. The spectrum of composite fields with masses below that scale is assumed to consist of spin-zero and spin-one fields, and the interactions among these particles and those of the Standard Model can be described by a $SU(2)_L \times SU(2)_R / SU(2)_{L+R}$ effective chiral

Lagrangian. Specifically, the composite fields included here are two scalars, h and H, one pseudoscalar η, a vector triplet V_μ^a and an axial vector triplet A_μ^a. The lightest scalar, h, is taken to be the newly discovered state at the LHC, with mass near 126 GeV. We will also assume that only h couples directly to the SM fermions, but H and η do not. In this scenario, in general one must include a deviation of the Higgs-fermion coupling with respect to the SM, which is parametrized here in terms of a coupling we call a_{hff}. This coupling is constrained from the requirement of good asymptotic behavior for the scattering of two longitudinal SM gauge bosons into a SM fermion pair.

Our main goal within this framework is to study the effect of the composite particles in the decay $h \to \gamma\gamma$. We found this rate to be consistent with the LHC observations provided the ratio between the composite vector and axial vector masses falls in a narrow range $M_V/M_A \sim 0.84$.

For consistency, we must check that the extra particles in the spectrum do not create an inconsistency with the high precision data that restrict the oblique parameters S and T. We found that the constraints on the T parameter at 95%C.L., together with the previously mentioned requirement of the $h \to \gamma\gamma$ decay rate, restrict the axial vector masses to be in the range $1.76 \text{ TeV} \lesssim M_A \lesssim 2.15 \text{ TeV}$. In addition, consistency with the experimental value on the S parameter requires the presence of a modified $W^3 - B^0$ mixing, which we parametrize in terms of a coupling c_{WB}. We find that a non-zero value for this coupling is necessary. The precise value depends on the masses M_V and M_A, but within the ranges quoted above, c_{WB} is between 0.1 and 0.3.

We also found that the T and S parameters have low sensitivity to the masses of the scalar and pseudoscalar composites, because the dominant contributions to T and S arise from quartic divergent terms, which only depend on the heavy vector and axial vector masses, not on the scalars. Consequently, from the point of view of the T and S values, the masses of these fields are not restricted.

In summary, we find that composite vectors and axial vectors do have an important effect on $h \to \gamma\gamma$, and their masses can be found such that the T and S parameters stay within their experimental bounds. However, one does require an extra $W^3 - B^0$ mixing, which in any case can be included in the Lagrangian still respecting all the symmetries. We also find that modified scalar-fermion couplings may appear, in order to preserve unitarity in the scattering of gauge fields into themselves and into fermion pairs.

Note that we find quartic and quadratic divergences in both T and S, while deconstructed models only yield logarithmic divergences for both parameters. This is due to the kinetic mixings between the SM gauge bosons and the heavy spin-one fields, which modify their propagators, introducing different loop contributions to the oblique parameters. Also worth mentioning is that we did not include composite fermions below the cutoff scale $\Lambda \sim 3$ TeV, which may affect the oblique T and S parameters as well. An extension of the model could include composite quarks, a fourth quark generation and/or vector-like quarks. Their effects on the oblique parameters and on the $h \to \gamma\gamma$ decay rate may be worth studying. Since the inclusion of extra quarks give a positive contribution to the T parameter as shown in Refs.[19, 21, 33, 73], we expect that an extension of the quark sector will increase the upper bound on the axial vector mass obtained from oblique parameter constraints, because the T parameter takes negative values when the heavy axial vector mass is increased. Addressing all these issues requires additional and careful analysis that we have left outside the scope of this work.

Acknowledgments

This work was supported in part by Conicyt (Chile) grant ACT-119 “Institute for advanced studies in Science and Technology”. C.D. also received support from Fondecyt (Chile) grant No. 1130617, and A.Z. from Fondecyt grant No. 1120346 and Conicyt grant ACT-91 “Southern Theoretical Physics Laboratory” .

A Spontaneously broken $SU(2)_L \times SU(2)_C \times SU(2)_D \times U(1)_Y$ gauge theory

Let us consider a theory with a gauge group of 4 sites, $SU(2)_L \times SU(2)_C \times SU(2)_D \times U(1)_Y$. We will assume that the interactions at some energy scale above a few TeV will cause the condensation of fermion bilinears, in a way somewhat analogous to what happens in QCD at the chiral symmetry breaking scale. The gauge symmetry is thus spontaneously broken to $U(1)_{em}$. The dynamical fields that are left below the symmetry breaking scale will obey an effective non-linear sigma model Lagrangian of the form:

$$\mathcal{L} = \mathcal{L}_{gauge} + \mathcal{L}_{\chi}^{gauge} - V\left(\Sigma_{LC}, \Sigma_{CD}, \Sigma_{DY}\right), \tag{A.1}$$

where $\mathcal{L}_{gauge}$ is the Lagrangian of the gauge fields, $\mathcal{L}_{\chi}^{gauge}$ contains the kinetic terms for the Higgs fields that will break the gauge symmetry when the Higgses acquire vacuum expectation values, and $V\left(\Sigma_{LC}, \Sigma_{CD}, \Sigma_{DY}\right)$ is the Higgs interaction potential. They are given by:

$$\mathcal{L}_{gauge} = -\sum_I \frac{1}{2g_I^2}\left\langle \omega_{\mu\nu}^I \omega^{\mu\nu I}\right\rangle, \quad \text{with } I = L,\ C,\ D,\ Y, \tag{A.2}$$

$$\begin{aligned}\mathcal{L}_{\chi}^{gauge} &= 2v_{LC}^2\left\langle D_\mu \Sigma_{LC} D^\mu \Sigma_{LC}^\dagger\right\rangle + 2v_{CD}^2\left\langle D_\mu \Sigma_{CD} D^\mu \Sigma_{CD}^\dagger\right\rangle \\ &+2v_{DY}^2\left\langle D_\mu \Sigma_{DY} D^\mu \Sigma_{DY}^\dagger\right\rangle,\end{aligned} \tag{A.3}$$

and

$$\begin{aligned}V\left(\Sigma_{LC}, \Sigma_{CD}, \Sigma_{DY}\right) = &-\frac{\mu_1^2 v_{LC}^2}{2}\left\langle \Sigma_{LC}\Sigma_{LC}^\dagger\right\rangle - \frac{\mu_2^2 v_{CD}^2}{2}\left\langle \Sigma_{CD}\Sigma_{CD}^\dagger\right\rangle - \frac{\mu_3^2 v_{DY}^2}{2}\left\langle \Sigma_{DY}\Sigma_{DY}^\dagger\right\rangle \\ &+\frac{\lambda_1 v_{LC}^4}{4}\left(\left\langle \Sigma_{LC}\Sigma_{LC}^\dagger\right\rangle\right)^2 + \frac{\lambda_2 v_{CD}^4}{4}\left(\left\langle \Sigma_{CD}\Sigma_{CD}^\dagger\right\rangle\right)^2 \\ &+\frac{\lambda_3 v_{DY}^4}{4}\left(\left\langle \Sigma_{DY}\Sigma_{DY}^\dagger\right\rangle\right)^2 + \kappa_1 v_{CD}^2 v_{LC}^2\left\langle \Sigma_{CD}\Sigma_{LC}^\dagger\Sigma_{LC}\Sigma_{CD}^\dagger\right\rangle \\ &+\kappa_2 v_{LC}^2 v_{DY}^2\left\langle \Sigma_{DY}\Sigma_{LC}^\dagger\Sigma_{LC}\Sigma_{DY}^\dagger\right\rangle + \kappa_3 v_{CD}^2 v_{DY}^2\left\langle \Sigma_{DY}\Sigma_{CD}^\dagger\Sigma_{CD}\Sigma_{DY}^\dagger\right\rangle.\end{aligned} \tag{A.4}$$

The covariant derivates are defined as:

$$D_\mu \Sigma_{IJ} = \partial_\mu \Sigma_{IJ} - i\omega_\mu^I \Sigma_{IJ} + i\Sigma_{IJ}\omega_\mu^J, \tag{A.5}$$

where $\omega^I_\mu = (W_\mu, \widetilde{v}_\mu, \widetilde{a}_\mu, B_\mu)$ with

$$B_\mu = \frac{g'}{2} B^0_\mu \tau^3, \quad W_\mu = \frac{g}{2} W^a_\mu \tau^a, \quad v_\mu = \frac{g_C}{2} v^a_\mu \tau^a \quad a_\mu = \frac{g_C}{2} a^a_\mu \tau^a, \tag{A.6}$$

where it has been assumed that $g_C = g_D$ and the indices I, J stand for $I, J = L, C, D, Y$. In turn, the field strength tensors are generically given by:

$$\omega^I_{\mu\nu} = \partial_\mu \omega^I_\nu - \partial_\nu \omega^I_\mu - i \left[\omega^I_\mu, \omega^I_\nu\right] . \tag{A.7}$$

To ensure the correct normalization for the Goldstone bosons kinetic terms, Σ_{LC}, Σ_{DY} and Σ_{CD} are defined as:

$$\Sigma_{LC} = \left(1 + \frac{\eta - \frac{1}{\sqrt{2}} h + \frac{1}{\sqrt{2}} H}{4 v_{LC}}\right) U_{LC}, \quad \text{with } \; U_{LC} = \exp\left[\frac{i}{4 v_{LC}} \left(\pi - \frac{1}{\sqrt{2}} \sigma + \frac{1}{\sqrt{2}} \rho\right)\right], \tag{A.8}$$

$$\Sigma_{DY} = \left(1 + \frac{-\eta - \frac{1}{\sqrt{2}} h + \frac{1}{\sqrt{2}} H}{4 v_{DY}}\right) U_{DY}, \quad \text{with } \; U_{DY} = \exp\left[\frac{i}{4 v_{DY}} \left(-\pi - \frac{1}{\sqrt{2}} \sigma + \frac{1}{\sqrt{2}} \rho\right)\right], \tag{A.9}$$

$$\Sigma_{CD} = \left(1 + \frac{h + H}{4 v_{CD}}\right) U_{CD}, \quad \text{with } \; U_{CD} = \exp\left[\frac{i}{4 v_{CD}} (\sigma + \rho)\right], \quad v_{LC} = v_{DY}, \tag{A.10}$$

where $\pi = \pi^a \tau^a$, $\sigma = \sigma^a \tau^a$ and $\rho = \rho^a \tau^a$, being π^a, σ^a and ρ^a the Goldstone bosons associated with the SM gauge bosons, the heavy vectors and heavy axial vectors, respecttively, and τ^a the usual Pauli matrices. In turn, h and H are the massive scalars and η is the massive pseudoscalar. The three Higgs doublets acquire vacuum expectation values, thus causing the spontaneous breaking of the $SU(2)_L \times SU(2)_C \times SU(2)_D \times U(1)_Y$ local symmetry down to $U(1)_{\text{em}}$, while the global group $G = SU(2)_L \times SU(2)_C \times SU(2)_D \times SU(2)_R$ is broken to the diagonal subgroup $H = SU(2)_{L+C+D+R}$. The Goldstone boson fields U_{IJ} can be put in the form:

$$U_{IJ} = \xi_I \xi^\dagger_J, \quad \text{where } \; U_{IJ} \in \frac{SU(2)_I \times SU(2)_J}{H}, \; I, J = L, C, D, Y. \tag{A.11}$$

These ξ_I transform under the full $SU(2)_L \times SU(2)_C \times SU(2)_D \times U(1)_Y$ as $\xi_I \to g_I \xi_I h^\dagger$. Choosing a gauge transformation $g_I = \xi^\dagger_I$ we can transfer the would-be Goldstone bosons to degrees of freedom of the gauge fields:

$$U_{IJ} \to \xi^\dagger_I U_{IJ} \xi_J = 1, \qquad \omega^I_\mu \to \xi^\dagger_I \omega^I_\mu \xi_I + i \xi^\dagger_I \partial_\mu \xi_I = \Omega^\mu_I, \tag{A.12}$$

and the Lagrangian of Eq. (A.3) reduces to:

$$\begin{aligned}
\mathcal{L}^{gauge}_\chi = {} & 2 v^2_{LC} \left(1 + \frac{\eta - \frac{1}{\sqrt{2}} h + \frac{1}{\sqrt{2}} H}{4 v_{LC}}\right)^2 \left\langle \left(\Omega^L_\mu - \Omega^C_\mu\right)^2 \right\rangle \\
& + 2 v^2_{LC} \left(1 + \frac{-\eta - \frac{1}{\sqrt{2}} h + \frac{1}{\sqrt{2}} H}{4 v_{LC}}\right)^2 \left\langle \left(\Omega^D_\mu - \Omega^Y_\mu\right)^2 \right\rangle \\
& + 2 v^2_{CD} \left(1 + \frac{h + H}{4 v_{CD}}\right)^2 \left\langle \left(\Omega^C_\mu - \Omega^D_\mu\right)^2 \right\rangle + \frac{1}{2} \partial_\mu h \partial^\mu h + \frac{1}{2} \partial_\mu H \partial^\mu H + \frac{1}{2} \partial_\mu \eta \partial^\mu \eta .
\end{aligned} \tag{A.13}$$

Specifically, we will do a partial gauge fixing resulting in $\xi_Y = \xi_L^\dagger = e^{i\pi/4 v_{LC}}$ and $\xi_C = \xi_D = 1$, which implies that $\sigma = \rho = 0$ and $U_{YD} = U_{CL}$. This gauge fixing corresponds to the unitary gauge where the Goldstone boson triplets σ and ρ are absorbed as longitudinal modes of Ω_μ^C and Ω_μ^D. These fields now transform under $SU(2)_L \times SU(2)_R$ according to:

$$\Omega_\mu^{C,D} \to h\Omega_\mu^{C,D} h^\dagger + ih\partial_\mu h^\dagger. \tag{A.14}$$

The Ω_μ^C and Ω_μ^D can be decomposed with respect to parity as:

$$\Omega_\mu^C = v_\mu + a_\mu, \qquad \Omega_\mu^D = v_\mu - a_\mu, \tag{A.15}$$

so that under $SU(2)_L \times SU(2)_R$ one has the following transformations:

$$v_\mu \to h v_\mu h^\dagger + ih\partial_\mu h^\dagger, \qquad a_\mu \to h a_\mu h^\dagger. \tag{A.16}$$

Defining

$$v_{\mu\nu} = \partial_\mu v_\nu - \partial_\nu v_\mu - i\left[v_\mu, v_\nu\right] \quad \text{and} \quad D_\mu^V a_\nu = \partial_\mu a_\nu - i\left[v_\mu, a_\nu\right], \tag{A.17}$$

we can write the interactions of the gauge sector of Eq. (A.2) in the form [46, 48]:

$$\mathcal{L}_{gauge} = \mathcal{L}_{gauge,SM} - \frac{1}{2g_C^2}\left[\left\langle \left(v_{\mu\nu} - i\left[a_\mu, a_\nu\right]\right)^2 \right\rangle + \left\langle \left(D_\mu^V a_\nu - D_\nu^V a_\mu\right)^2 \right\rangle\right]. \tag{A.18}$$

Now, due to mixing with the SM fields, v_μ and a_μ are not mass eigenstates. The vector and axial vector mass eigenstates as V_μ and A_μ, respectively, are actually given by the following relations [46, 48]:

$$V_\mu = v_\mu - i\Gamma_\mu, \qquad A_\mu = a_\mu + \frac{\kappa}{2} u_\mu, \tag{A.19}$$

where κ will be determined below, and Γ_μ is defined as:

$$\Gamma_\mu \equiv \frac{1}{2i}\left(\Omega_\mu^Y + \Omega_\mu^L\right) = \frac{1}{2}\left[u^\dagger\left(\partial_\mu - iB_\mu\right)u + u\left(\partial_\mu - iW_\mu\right)u^\dagger\right]. \tag{A.20}$$

Considering these definitions, the strength tensors satisfy the following identities:

$$v_{\mu\nu} = V_{\mu\nu} - i\left[V_\mu, V_\nu\right] + \frac{i}{4}\left[u_\mu, u_\nu\right] + \frac{1}{2}\left(uW_{\mu\nu}u^\dagger + u^\dagger B_{\mu\nu}u\right), \tag{A.21}$$

$$a_{\mu\nu} = A_{\mu\nu} - \frac{\kappa}{2}u_{\mu\nu} - i\left[V_\mu, A_\nu - \frac{\kappa}{2}u_\nu\right] + i\left[V_\nu, A_\mu - \frac{\kappa}{2}u_\mu\right], \tag{A.22}$$

where

$$W_{\mu\nu} = \partial_\mu W_\nu - \partial_\nu W_\mu - i\left[W_\mu, W_\nu\right], \qquad B_{\mu\nu} = \partial_\mu B_\nu - \partial_\nu B_\mu, \tag{A.23}$$

$$V_{\mu\nu} = \nabla_\mu V_\nu - \nabla_\nu V_\mu = \partial_\mu V_\nu - \partial_\nu V_\mu + \left[\Gamma_\mu, V_\nu\right] - \left[\Gamma_\nu, V_\mu\right], \tag{A.24}$$

$$A_{\mu\nu} = \nabla_\mu A_\nu - \nabla_\nu A_\mu = \partial_\mu A_\nu - \partial_\nu A_\mu + \left[\Gamma_\mu, A_\nu\right] - \left[\Gamma_\nu, A_\mu\right], \tag{A.25}$$

$$u_{\mu\nu} = \partial_\mu u_\nu - \partial_\nu u_\mu + \left[\Gamma_\mu, u_\nu\right] - \left[\Gamma_\nu, u_\mu\right]. \tag{A.26}$$

With these definitions and the aforementioned gauge fixing, the symmetry breaking sector of the Lagrangian becomes:

$$
\begin{aligned}
\mathcal{L}_{\chi}^{gauge} &= 4v_{LC}^2\left(1+\frac{H-h}{2\sqrt{2}v_{LC}}+\frac{H^2+h^2-2hH}{32v_{LC}^2}+\frac{\eta^2}{16v_{LC}^2}\right)\\
&\times\left[\langle V_\mu V^\mu\rangle+\langle A_\mu A^\mu\rangle+\left(\frac{1-\kappa}{2}\right)^2\langle u_\mu u^\mu\rangle+(1-\kappa)\langle A_\mu u^\mu\rangle\right]\\
&+4v_{LC}\eta\left(1+\frac{H-h}{4\sqrt{2}v_{LC}}\right)\left[\langle V_\mu A^\mu\rangle+\left(\frac{1-\kappa}{2}\right)\langle V_\mu u^\mu\rangle\right]\\
&+8v_{CD}^2\left(1+\frac{h+H}{2v_{CD}}+\frac{h^2+2hH+H^2}{16v_{CD}^2}\right)\left[\langle A_\mu A^\mu\rangle+\frac{\kappa^2}{4}\langle u_\mu u^\mu\rangle-\kappa\langle A_\mu u^\mu\rangle\right]\\
&+\frac{1}{2}\partial_\mu\eta\partial^\mu\eta+\frac{1}{2}\partial_\mu h\partial^\mu h+\frac{1}{2}\partial_\mu H\partial^\mu H,
\end{aligned}
\tag{A.27}
$$

where one defines:

$$
u_\mu\equiv\Omega_\mu^Y-\Omega_\mu^L=iu^\dagger D_\mu U u^\dagger,\quad\text{with}\quad U=u^2=e^{\frac{i}{v}\pi^a\tau^a}\quad\text{and}\quad D_\mu U=\partial_\mu U-iB_\mu U+iUW_\mu,
\tag{A.28}
$$

and where D_μ is a covariant derivative containing the SM gauge fields only.

With the further replacement $V_\mu\to\frac{g_C}{\sqrt{2}}V_\mu$, $A_\mu\to\frac{g_C}{\sqrt{2}}A_\mu$, the Gauge sector of the Lagrangian becomes:

$$
\begin{aligned}
\mathcal{L}_{gauge} &= \mathcal{L}_{gauge,SM}-\frac{1}{4}\langle V_{\mu\nu}V^{\mu\nu}\rangle-\frac{1}{4}\langle A_{\mu\nu}A^{\mu\nu}\rangle-\frac{i\left(1-\kappa^2\right)}{8g_C^2}\left\langle[u^\mu,u^\nu]\left(uW_{\mu\nu}u^\dagger+u^\dagger B_{\mu\nu}u\right)\right\rangle\\
&-\frac{\kappa^2}{8g_C^2}\langle u_{\mu\nu}u^{\mu\nu}\rangle+\frac{\left(1-\kappa^2\right)^2}{32g_C^2}\langle[u_\mu,u_\nu][u^\mu,u^\nu]\rangle-\frac{1}{2\sqrt{2}g_C}\left\langle V^{\mu\nu}\left(uW_{\mu\nu}u^\dagger+u^\dagger B_{\mu\nu}u\right)\right\rangle\\
&+\frac{\kappa}{2\sqrt{2}g_C}\langle u_{\mu\nu}A^{\mu\nu}\rangle-\frac{i\left(1-\kappa^2\right)}{4\sqrt{2}g_C}\langle V^{\mu\nu}[u_\mu,u_\nu]\rangle+\frac{i\kappa^2}{2\sqrt{2}g_C}\langle u_{\mu\nu}[V^\mu,u^\nu]\rangle\\
&-\frac{i\kappa}{2\sqrt{2}g_C}\left\langle\left(uW_{\mu\nu}u^\dagger+u^\dagger B_{\mu\nu}u\right)[A^\mu,u^\nu]\right\rangle+\frac{\kappa\left(1-\kappa^2\right)}{4\sqrt{2}g_C}\langle[u_\mu,u_\nu][A^\mu,u^\nu]\rangle\\
&-\frac{1}{8g_C^2}\left\langle\left(uW_{\mu\nu}u^\dagger+u^\dagger B_{\mu\nu}u\right)\left(uW^{\mu\nu}u^\dagger+u^\dagger B^{\mu\nu}u\right)\right\rangle-\frac{i\kappa}{2}\langle u_{\mu\nu}[V^\mu,A^\nu]\rangle\\
&-\frac{1-\kappa^2}{8}\langle[V_\mu,V_\nu][u^\mu,u^\nu]\rangle+\frac{\kappa^2}{8}\langle[V_\mu,u_\nu]([V^\mu,u^\nu]-[V^\nu,u^\mu])\rangle-\frac{i\kappa}{2}\langle V_{\mu\nu}[A^\mu,u^\nu]\rangle\\
&-\frac{1-\kappa^2}{8}\langle[A_\mu,A_\nu][u^\mu,u^\nu]\rangle+\frac{\kappa^2}{8}\langle[A_\mu,u_\nu]([A^\mu,u^\nu]-[A^\nu,u^\mu])\rangle-\frac{i\kappa}{2}\langle A_{\mu\nu}[V^\mu,u^\nu]\rangle\\
&+\frac{i}{4}\left\langle[V^\mu,V^\nu]\left(uW_{\mu\nu}u^\dagger+u^\dagger B_{\mu\nu}u\right)\right\rangle+\frac{i}{4}\left\langle[A^\mu,A^\nu]\left(uW_{\mu\nu}u^\dagger+u^\dagger B_{\mu\nu}u\right)\right\rangle\\
&+\frac{ig_C}{2\sqrt{2}}\langle V^{\mu\nu}[V_\mu,V_\nu]\rangle+\frac{ig_C}{2\sqrt{2}}\langle V_{\mu\nu}[A^\mu,A^\nu]\rangle+\frac{ig_C}{\sqrt{2}}\langle A_{\mu\nu}[V^\mu,A^\nu]\rangle\\
&-\frac{\kappa g_C}{2\sqrt{2}}\langle[A_\mu,A_\nu][A^\mu,u^\nu]\rangle-\frac{\kappa g_C}{2\sqrt{2}}\langle[V_\mu,u_\nu]([V^\mu,A^\nu]-[V^\nu,A^\mu])\rangle\\
&+\frac{g_C^2}{8}\langle[V_\mu,V_\nu][V^\mu,V^\nu]\rangle+\frac{g_C^2}{4}\langle[V_\mu,V_\nu][A^\mu,A^\nu]\rangle+\frac{g_C^2}{8}\langle[A_\mu,A_\nu][A^\mu,A^\nu]\rangle\\
&-\frac{\kappa g_C}{2\sqrt{2}}\langle[V_\mu,V_\nu][A^\mu,u^\nu]\rangle+\frac{g_C^2}{4}\langle[V_\mu,A_\nu]([V^\mu,A^\nu]-[V^\nu,A^\mu])\rangle\,.
\end{aligned}
\tag{A.29}
$$

where the correct normalization of the kinetic terms of the heavy spin-1 resonances implies [46, 48]:

$$V_\mu = \frac{1}{\sqrt{2}}\tau^a V^a_\mu, \qquad\qquad A_\mu = \frac{1}{\sqrt{2}}\tau^a A^a_\mu, \tag{A.30}$$

while the symmetry breaking sector of the Lagrangian takes the following form:

$$\begin{aligned}\mathcal{L}^{gauge}_\chi = {} & 4v^2_{LC}\left(1+\frac{H-h}{2\sqrt{2}v_{LC}}+\frac{H^2+h^2-2hH}{32v^2_{LC}}+\frac{\eta^2}{16v^2_{LC}}\right) \\ & \times\left[\frac{g^2_C}{2}\langle V_\mu V^\mu\rangle+\frac{g^2_C}{2}\langle A_\mu A^\mu\rangle+\left(\frac{1-\kappa}{2}\right)^2\langle u_\mu u^\mu\rangle+\frac{2g_C}{\sqrt{2}}\left(\frac{1-\kappa}{2}\right)\langle A_\mu u^\mu\rangle\right] \\ & +4v_{LC}\eta\left(1+\frac{H-h}{4\sqrt{2}v_{LC}}\right)\left[\frac{g^2_C}{2}\langle V_\mu A^\mu\rangle+\frac{g_C}{\sqrt{2}}\left(\frac{1-\kappa}{2}\right)\langle V_\mu u^\mu\rangle\right] \\ & +8v^2_{CD}\left(1+\frac{h+H}{2v_{CD}}+\frac{h^2+2hH+H^2}{16v^2_{CD}}\right)\left[\frac{g^2_C}{2}\langle A_\mu A^\mu\rangle+\frac{\kappa^2}{4}\langle u_\mu u^\mu\rangle-\frac{\kappa g_C}{\sqrt{2}}\langle A_\mu u^\mu\rangle\right] \\ & +\frac{1}{2}\partial_\mu h\partial^\mu h+\frac{1}{2}\partial_\mu H\partial^\mu H+\frac{1}{2}\partial_\mu\eta\partial^\mu\eta. \end{aligned} \tag{A.31}$$

Since V_μ and A_μ define the mass eigenstates, the term $A_\mu u^\mu$ should be absent in the previous expression, yielding the following relation:

$$\left(\frac{1-\kappa}{2}\right)v^2_{LC}-\kappa v^2_{CD}=0. \tag{A.32}$$

In addition, the requirement of having the correct W gauge boson mass implies:

$$\left(\frac{1-\kappa}{2}\right)^2 v^2_{LC}+\frac{\kappa^2}{2}v^2_{CD}=\frac{v^2}{16}. \tag{A.33}$$

The previous equations have the following solutions:

$$v_{LC}=\frac{v}{2\sqrt{1-\kappa}}, \quad v_{CD}=\frac{v}{2\sqrt{2\kappa}}, \quad \text{with} \;\; 0<\kappa<1. \tag{A.34}$$

Then, from the expressions (A.31) and (A.34) it follows that the masses of V^a_μ and A^a_μ are determined by the parameters g_C and κ as:

$$M_V=\frac{g_C v}{\sqrt{1-\kappa}}, \qquad M_A=\frac{M_V}{\sqrt{\kappa}}. \tag{A.35}$$

We now see that the diagonalization procedure determines κ in Eq. (A.19) as the mass ratio $\kappa = M^2_V/M^2_A$. On the other hand, the strength of the gauge coupling g_C determines the absolute value of these masses. The coupling g_C also controls the kinetic mixing between V^a_μ and the SM gauge bosons, while the kinetic mixing between A^a_μ and the SM gauge bosons is controlled by both κ and g_C, as seen in Eq. (A.29).

Consequently the Lagrangian that describes the interactions among the composite spin zero fields, the composite spin one fields and the SM gauge bosons and SM Goldstone bosons is given by:

$$\mathcal{L}=\mathcal{L}_{gauge}+\mathcal{L}^{gauge}_\chi-V\left(\Sigma_{LC},\Sigma_{CD},\Sigma_{DY}\right). \tag{A.36}$$

This same Lagrangian is described in Eq. (2.33), where the scalar potential has been expanded to quadratic factors of the scalar fields. We did not include the cubic and quartic scalar interactions in Eq. (2.33) as they are irrelevant to our calculations of the $h \to \gamma\gamma$ decay rate and the oblique T and S parameters.

B Calculation of the T and S parameters.

The T parameter is defined as [81–84]:

$$T = \frac{\widehat{T}}{\alpha_{em}\left(m_Z\right)}, \qquad \widehat{T} = \frac{\Pi_{33}\left(0\right) - \Pi_{11}\left(0\right)}{M_W^2}, \tag{B.1}$$

where $\Pi_{11}\left(0\right)$ and $\Pi_{33}\left(0\right)$ are the vacuum polarization amplitudes for loop diagrams having gauge bosons W_μ^1, W_μ^1 and W_μ^3, W_μ^3 in the external lines, respectively. These vacuum polarization amplitudes are evaluated at $q^2 = 0$, where q the external momentum. The one-loop diagrams that give contributions to the T parameter should include the hypercharge gauge boson B_μ^0 since the g' coupling is one of the sources of the breaking of the custodial symmetry. The other source of custodial symmetry breaking comes from the difference between up and down type quark Yukawa couplings. The corresponding Feynman diagrams are shown in Figure 4 and we computed them in the Landau Gauge for the SM gauge bosons and Goldstone bosons, where the global $SU(2)_L \times U(1)_Y$ symmetry is preserved. Regarding the heavy composite spin-1 resonances, we use the Unitary Gauge for their propagators since the Lagrangian given in Eq. (2.33) does not include the Goldstone bosons associated to the longitudinal components of these heavy parity even and parity odd spin-1 resonances. From the Feynman diagrams shown in Figure 4, it follows that the $\widehat{T}$ parameter is given by:

$$\begin{aligned}
\widehat{T} = {} & \widehat{T}_{(\pi^2 B^0)} + \widehat{T}_{(V^3 B^0,\pi^2)} + \widehat{T}_{(V^3 B^0 V^3,\pi^2)} + \widehat{T}_{(V^2 B^0)} + \widehat{T}_{(A^2 B^0)} + \widehat{T}_{(V^3 B^0,V^2)} \\
& + \widehat{T}_{(A^3 B^0,A^2)} + \widehat{T}_{(V^3 B^0 V^3,V^2)} + \widehat{T}_{(A^3 B^0 A^3,A^2)} + \widehat{T}_{(V^3 B^0,A^2)} + \widehat{T}_{(A^3 B^0,V^2)} \\
& + \widehat{T}_{(V^3 B^0 V^3,A^2)} + \widehat{T}_{(A^3 B^0 A^3,V^2)} + \widehat{T}_{(V^3 B^0 A^3,V^2)} + \widehat{T}_{(V^3 B^0 A^3,A^2)} \\
& + \widehat{T}_{(B^0)} + \widehat{T}_{(V^3 B^0 V^3)} + \widehat{T}_{(A^3 B^0 A^3)} + \widehat{T}_{(V^3 B^0 A^3)} + \widehat{T}_{(V^3 - B^0)} + \widehat{T}_{(hB^0)} + \widehat{T}_{(HB^0)} \\
& + \widehat{T}_{(\eta,V^3 B^0 V^3)} + \widehat{T}_{(h,A^3 B^0 A^3)} + \widehat{T}_{(H,A^3 B^0 A^3)} + \widehat{T}_{(h,A^3 B^0)} + \widehat{T}_{(H,A^3 B^0)},
\end{aligned} \tag{B.2}$$

where the different one-loop contributions to the $\widehat{T}$ parameter are:

$$\widehat{T}_{(\pi^2 B^0)} \simeq -\frac{3\alpha_{em}}{16\pi\cos^2\theta_W}\ln\left(\frac{\Lambda^2}{M_W^2}\right) - \frac{3\alpha_{em}\left(f_V g_V - \frac{1}{2}f_A^2\right)^2}{32\pi v^4\cos^2\theta_W}\Lambda^4 + \frac{3\alpha_{em}\left(f_V g_V - \frac{1}{2}f_A^2\right)}{8\pi v^2\cos^2\theta_W}\Lambda^2, \tag{B.3}$$

$$\begin{aligned}
\widehat{T}_{(V^3 B^0,\pi^2)} \simeq {} & -\frac{3\alpha_{em} f_V g_V\left(f_V g_V - \frac{1}{2}f_A^2\right)}{16\pi v^4\cos^2\theta_W}\Lambda^4 \\
& -\frac{3\alpha_{em} f_V g_V}{8\pi v^2\cos^2\theta_W}\left[1 - \left(f_V g_V - \frac{1}{2}f_A^2\right)\frac{M_V^2}{v^2}\right]\left[\Lambda^2 - M_V^2\ln\left(\frac{\Lambda^2 + M_V^2}{M_V^2}\right)\right],
\end{aligned} \tag{B.4}$$

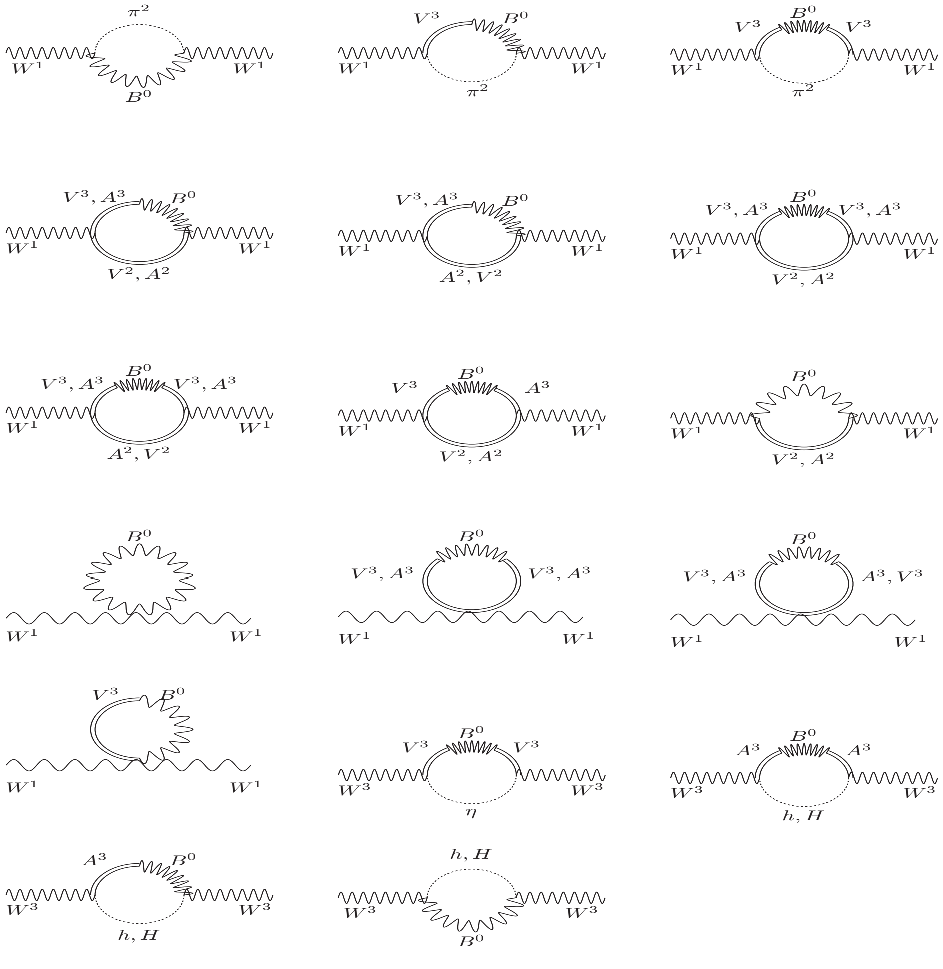

Figure 4. One loop Feynman diagrams contributing to the T parameter.

$$\widehat{T}_{(V^3B^0V^3,\pi^2)} \simeq -\frac{3\alpha_{em} f_V^2 g_V^2}{32\pi v^4 \cos^2\theta_W}\left[\Lambda^4 - 4M_V^2\Lambda^2 + 6M_V^4 \ln\left(\frac{\Lambda^2+M_V^2}{M_V^2}\right) - \frac{2M_V^4\Lambda^2}{\Lambda^2+M_V^2}\right], \tag{B.5}$$

$$\widehat{T}_{(V^2B^0)} \simeq \frac{3\alpha_{em}\left(1-\kappa^2\right)^2 f_V^2}{128\pi v^2 M_V^2 \cos^2\theta_W}\Lambda^4 + \frac{3\alpha_{em}\left[\left(1-\kappa^2\right)f_V - 2g_V\right]^2}{64\pi v^2\cos^2\theta_W}\left[\Lambda^2 - M_V^2 \ln\left(\frac{\Lambda^2+M_V^2}{M_V^2}\right)\right], \tag{B.6}$$

$$\widehat{T}_{(A^2B^0)} \simeq \frac{3\alpha_{em} f_A^2}{128\pi v^2 M_A^2 \cos^2\theta_W}\Lambda^4 + \frac{3\alpha_{em} f_A^2}{64\pi v^2\cos^2\theta_W}\left[\Lambda^2 - M_A^2 \ln\left(\frac{\Lambda^2+M_A^2}{M_A^2}\right)\right], \tag{B.7}$$

$$\begin{aligned}\widehat{T}_{(V^3B^0,V^2)} \simeq \frac{3\alpha_{em} f_V}{64\pi v^2 M_V^2 \cos^2\theta_W} \Bigg\{ & \left(1-\kappa^2\right) f_V \Lambda^4 - 2\left[4g_V - \left(1-\kappa^2\right) f_V\right] M_V^2 \Lambda^2 \\ & +2\left[8g_V - 3\left(1-\kappa^2\right) f_V\right] M_V^4 \ln\left(\frac{\Lambda^2+M_V^2}{M_V^2}\right) - \frac{4\left[2g_V - \left(1-\kappa^2\right) f_V\right] M_V^4 \Lambda^2}{\Lambda^2+M_V^2} \Bigg\},\end{aligned} \tag{B.8}$$

$$\widehat{T}_{(A^3B^0,A^2)} \simeq -\frac{3\alpha_{em} f_A^2}{64\pi v^2 M_A^2 \cos^2\theta_W} \left[\Lambda^4 + 2M_A^2\Lambda^2 - 6M_A^4 \ln\left(\frac{\Lambda^2+M_A^2}{M_A^2}\right) + \frac{4M_A^4\Lambda^2}{\Lambda^2+M_A^2}\right], \tag{B.9}$$

$$\begin{aligned}\widehat{T}_{(V^3B^0V^3,V^2)} \simeq \frac{3\alpha_{em} f_V^2}{128\pi v^2 M_V^2 \cos^2\theta_W} \Bigg\{ & \Lambda^4 + 4M_V^2\Lambda^2 + 18M_V^4 \left[1 - \ln\left(\frac{\Lambda^2+M_V^2}{M_V^2}\right)\right] \\ & -2M_V^6 \frac{11\Lambda^2 + 9M_V^2}{\left(\Lambda^2+M_V^2\right)^2} \Bigg\},\end{aligned} \tag{B.10}$$

$$\begin{aligned}\widehat{T}_{(A^3B^0A^3,A^2)} \simeq \frac{3\alpha_{em} f_A^2}{128\pi v^2 M_A^2 \cos^2\theta_W} \Bigg\{ & \Lambda^4 + 4M_A^2\Lambda^2 + 18M_A^4 \left[1 - \ln\left(\frac{\Lambda^2+M_A^2}{M_A^2}\right)\right] \\ & -2M_A^6 \frac{11\Lambda^2 + 9M_A^2}{\left(\Lambda^2+M_A^2\right)^2} \Bigg\},\end{aligned} \tag{B.11}$$

$$\begin{aligned}\widehat{T}_{(V^3B^0,A^2)} \simeq \frac{3\alpha_{em} \kappa f_V f_A}{64\pi v^2 M_A^2 \cos^2\theta_W} \Bigg\{ & \Lambda^4 + 2\left(2M_A^2 - M_V^2\right)\Lambda^2 \\ & + \frac{2M_V^4\left(M_V^2 - 3M_A^2\right)}{M_V^2 - M_A^2} \ln\left(\frac{\Lambda^2+M_V^2}{M_V^2}\right) - \frac{4M_A^6}{M_A^2 - M_V^2} \ln\left(\frac{\Lambda^2+M_A^2}{M_A^2}\right) \Bigg\},\end{aligned} \tag{B.12}$$

$$\begin{aligned}\widehat{T}_{(A^3B^0,V^2)} \simeq -\frac{3\alpha_{em} \kappa f_A}{64\pi v^2 M_V^2 \cos^2\theta_W} \Bigg\{ & \left(1-\kappa^2\right) f_V \Lambda^4 \\ & + \left[4\left(\left(1-\kappa^2\right) f_V - 2g_V\right) M_V^2 - 2\left(1-\kappa^2\right) f_V M_A^2\right] \Lambda^2 \\ & - \frac{4\left(\left(1-\kappa^2\right) f_V - 2g_V\right) M_V^6}{M_V^2 - M_A^2} \ln\left(\frac{\Lambda^2+M_V^2}{M_V^2}\right) \\ & + \frac{\left[2\left(1-\kappa^2\right) f_V M_A^2 - 2\left(3\left(1-\kappa^2\right) f_V - 4g_V\right) M_V^2\right] M_A^4}{M_A^2 - M_V^2} \ln\left(\frac{\Lambda^2+M_A^2}{M_A^2}\right) \Bigg\},\end{aligned} \tag{B.13}$$

$$\begin{aligned}\widehat{T}_{(V^3B^0V^3,A^2)} \simeq\ & \frac{3\alpha_{em}\kappa^2 f_V^2}{128\pi v^2 M_A^2\cos^2\theta_W}\Biggl\{\Lambda^4+4\left(2M_A^2-M_V^2\right)\Lambda^2-\frac{2M_V^4\left(5M_A^2-M_V^2\right)\Lambda^2}{\left(M_A^2-M_V^2\right)\left(\Lambda^2+M_V^2\right)}\\ & +2M_V^4\frac{3M_V^4+15M_A^4-14M_A^2M_V^2}{\left(M_A^2-M_V^2\right)^2}\ln\left(\frac{\Lambda^2+M_V^2}{M_V^2}\right)\\ & -\frac{8M_A^8}{\left(M_A^2-M_V^2\right)^2}\ln\left(\frac{\Lambda^2+M_A^2}{M_A^2}\right)\Biggr\},\end{aligned} \tag{B.14}$$

$$\begin{aligned}\widehat{T}_{(A^3B^0A^3,V^2)} \simeq\ & \frac{3\alpha_{em}\kappa^2 f_A^2}{128\pi v^2 M_V^2\cos^2\theta_W}\Biggl\{\Lambda^4+4\left(2M_V^2-M_A^2\right)\Lambda^2-\frac{2M_A^4\left(5M_V^2-M_A^2\right)\Lambda^2}{\left(M_V^2-M_A^2\right)\left(\Lambda^2+M_A^2\right)}\\ & +2M_A^4\frac{3M_A^4+15M_V^4-14M_A^2M_V^2}{\left(M_A^2-M_V^2\right)^2}\ln\left(\frac{\Lambda^2+M_A^2}{M_A^2}\right)\\ & -\frac{8M_V^8}{\left(M_A^2-M_V^2\right)^2}\ln\left(\frac{\Lambda^2+M_V^2}{M_V^2}\right)\Biggr\},\end{aligned} \tag{B.15}$$

$$\begin{aligned}\widehat{T}_{(V^3B^0A^3,V^2)} \simeq\ & -\frac{3\alpha_{em}\kappa f_V f_A}{64\pi v^2 M_V^2\cos^2\theta_W}\Biggl\{\Lambda^4-2\left(M_A^2-3M_V^2\right)\Lambda^2\\ & +\frac{2M_A^6\left(M_A^2-5M_V^2\right)}{\left(M_A^2-M_V^2\right)^2}\ln\left(\frac{\Lambda^2+M_A^2}{M_A^2}\right)\\ & +2M_V^4\left[3-\frac{\left(M_A^2-5M_V^2\right)\left(3M_A^2-2M_V^2\right)}{\left(M_V^2-M_A^2\right)^2}\right]\ln\left(\frac{\Lambda^2+M_V^2}{M_V^2}\right)\\ & +\frac{8M_V^6\Lambda^2}{\left(M_V^2-M_A^2\right)\left(\Lambda^2+M_V^2\right)}\Biggr\},\end{aligned} \tag{B.16}$$

$$\begin{aligned}\widehat{T}_{(V^3B^0A^3,A^2)} \simeq\ & -\frac{3\alpha_{em}\kappa f_V f_A}{64\pi v^2 M_A^2\cos^2\theta_W}\Biggl\{\Lambda^4-2\left(M_V^2-3M_A^2\right)\Lambda^2\\ & +2M_A^4\left[3-\frac{\left(M_V^2-5M_A^2\right)\left(3M_V^2-2M_A^2\right)}{\left(M_V^2-M_A^2\right)^2}\right]\ln\left(\frac{\Lambda^2+M_A^2}{M_A^2}\right)\\ & +\frac{2M_V^6\left(M_V^2-5M_A^2\right)}{\left(M_A^2-M_V^2\right)^2}\ln\left(\frac{\Lambda^2+M_V^2}{M_V^2}\right)+\frac{8M_A^6\Lambda^2}{\left(M_A^2-M_V^2\right)\left(\Lambda^2+M_A^2\right)}\Biggr\},\end{aligned} \tag{B.17}$$

$$\widehat{T}_{(B^0)} \simeq -\frac{9\alpha_{em}g_V^2}{16\pi v^2\cos^2\theta_W}\Lambda^2, \tag{B.18}$$

$$\widehat{T}_{(V^3B^0V^3)} \simeq -\frac{9\alpha_{em}\left(1+\kappa^2\right)f_V^2}{64\pi v^2\cos^2\theta_W}\left[\Lambda^2-2M_V^2\ln\left(\frac{\Lambda^2+M_V^2}{M_V^2}\right)+\frac{\Lambda^2M_V^2}{\Lambda^2+M_V^2}\right], \tag{B.19}$$

$$\widehat{T}_{(A^3B^0A^3)} \simeq -\frac{9\alpha_{em}\left(1+\kappa^2\right)f_A^2}{64\pi v^2\cos^2\theta_W}\left[\Lambda^2-2M_A^2\ln\left(\frac{\Lambda^2+M_A^2}{M_A^2}\right)+\frac{\Lambda^2M_A^2}{\Lambda^2+M_A^2}\right], \tag{B.20}$$

$$\widehat{T}_{(V^3B^0A^3)} \simeq \frac{9\alpha_{em}\kappa f_V f_A}{16\pi v^2\cos^2\theta_W}\left[\Lambda^2-\frac{M_V^4}{M_V^2-M_A^2}\ln\left(\frac{\Lambda^2+M_V^2}{M_V^2}\right)-\frac{M_A^4}{M_A^2-M_V^2}\ln\left(\frac{\Lambda^2+M_A^2}{M_A^2}\right)\right] \tag{B.21}$$

$$\widehat{T}_{(V^3-B^0)} \simeq \frac{9\alpha_{em}f_Vg_V}{16\pi v^2\cos^2\theta_W}\left[\Lambda^2-M_V^2\ln\left(\frac{\Lambda^2+M_V^2}{M_V^2}\right)\right], \tag{B.22}$$

$$\widehat{T}_{(hB^0)} \simeq \frac{3\alpha_{em}\left[(1-\kappa)^{\frac{3}{2}}-2\kappa^{\frac{3}{2}}\right]^2}{128\pi\cos^2\theta_W}\ln\left(\frac{\Lambda^2}{m_h^2}\right), \tag{B.23}$$

$$\widehat{T}_{(HB^0)} \simeq \frac{3\alpha_{em}\left[(1-\kappa)^{\frac{3}{2}}+2\kappa^{\frac{3}{2}}\right]^2}{128\pi\cos^2\theta_W}\ln\left(\frac{\Lambda^2}{m_H^2}\right), \tag{B.24}$$

$$\begin{aligned}\widehat{T}_{(\eta,V^3B^0V^3)} \simeq{}& \frac{3\alpha_{em}f_V^2\left(1-\kappa\right)^2M_V^2}{64\pi v^2\left(M_V^2-m_\eta^2\right)\cos^2\theta_W}\left\{\frac{M_V^4-2M_V^2m_\eta^2}{M_V^2-m_\eta^2}\ln\left(\frac{\Lambda^2+M_V^2}{M_V^2}\right)\right.\\ &\left.-\frac{m_\eta^4}{m_\eta^2-M_V^2}\ln\left(\frac{\Lambda^2+m_\eta^2}{m_\eta^2}\right)-\frac{M_V^2\Lambda^2}{\Lambda^2+M_V^2}\right\},\end{aligned} \tag{B.25}$$

$$\begin{aligned}\widehat{T}_{(h,A^3B^0A^3)} \simeq{}& \frac{3\alpha_{em}\kappa\left(1-\kappa\right)\left(\sqrt{1-\kappa}+2\sqrt{\kappa}\right)^2f_A^2M_A^2}{128\pi v^2\left(M_A^2-m_h^2\right)\cos^2\theta_W}\left\{\frac{M_A^4-2M_A^2m_h^2}{M_A^2-m_h^2}\ln\left(\frac{\Lambda^2+M_A^2}{M_A^2}\right)\right.\\ &\left.-\frac{m_h^4}{m_h^2-M_A^2}\ln\left(\frac{\Lambda^2+m_h^2}{m_h^2}\right)-\frac{M_A^2\Lambda^2}{\Lambda^2+M_A^2}\right\},\end{aligned} \tag{B.26}$$

$$\begin{aligned}\widehat{T}_{(H,A^3B^0A^3)} \simeq{}& \frac{3\alpha_{em}\kappa\left(1-\kappa\right)\left(\sqrt{1-\kappa}-2\sqrt{\kappa}\right)^2f_A^2M_A^2}{128\pi v^2\left(M_A^2-m_H^2\right)\cos^2\theta_W}\left\{\frac{M_A^4-2M_A^2m_H^2}{M_A^2-m_H^2}\ln\left(\frac{\Lambda^2+M_A^2}{M_A^2}\right)\right.\\ &\left.-\frac{m_H^4}{m_H^2-M_A^2}\ln\left(\frac{\Lambda^2+m_H^2}{m_H^2}\right)-\frac{M_A^2\Lambda^2}{\Lambda^2+M_A^2}\right\},\end{aligned} \tag{B.27}$$

$$\begin{aligned}\widehat{T}_{(h,A^3B^0)} \simeq{}& \frac{3\alpha_{em}\sqrt{\kappa}\sqrt{1-\kappa}\left(\sqrt{1-\kappa}+2\sqrt{\kappa}\right)a_hf_AM_A}{16\sqrt{2}\pi v\cos^2\theta_W}\left\{\frac{M_A^2}{M_A^2-m_h^2}\ln\left(\frac{\Lambda^2+M_A^2}{M_A^2}\right)\right.\\ &\left.+\frac{m_h^2}{m_h^2-M_A^2}\ln\left(\frac{\Lambda^2+m_h^2}{m_h^2}\right)\right\},\end{aligned} \tag{B.28}$$

$$\widehat{T}_{(H,A^3B^0)} \simeq \frac{3\alpha_{em}\sqrt{\kappa}\sqrt{1-\kappa}\left(\sqrt{1-\kappa}+2\sqrt{\kappa}\right)a_h f_A M_A}{16\sqrt{2}\pi v\cos^2\theta_W}$$
$$\left[\frac{M_A^2}{M_A^2-m_H^2}\ln\left(\frac{\Lambda^2+M_A^2}{M_A^2}\right)+\frac{m_H^2}{m_H^2-M_A^2}\ln\left(\frac{\Lambda^2+m_H^2}{m_H^2}\right)\right]. \tag{B.29}$$

Now, considering the S parameter, it is defined as [81–84]:

$$S=\frac{4\sin^2\theta_W}{\alpha_{em}\left(m_Z\right)}\widehat{S}, \qquad \widehat{S}=\frac{g}{g'}\frac{d\Pi_{30}\left(q^2\right)}{dq^2}\bigg|_{q^2=0}, \tag{B.30}$$

where $\Pi_{30}\left(q^2\right)$ is the vacuum polarization amplitude for a loop diagram having W_μ^3 and B_μ in the external lines. As before, here q is the external momentum.

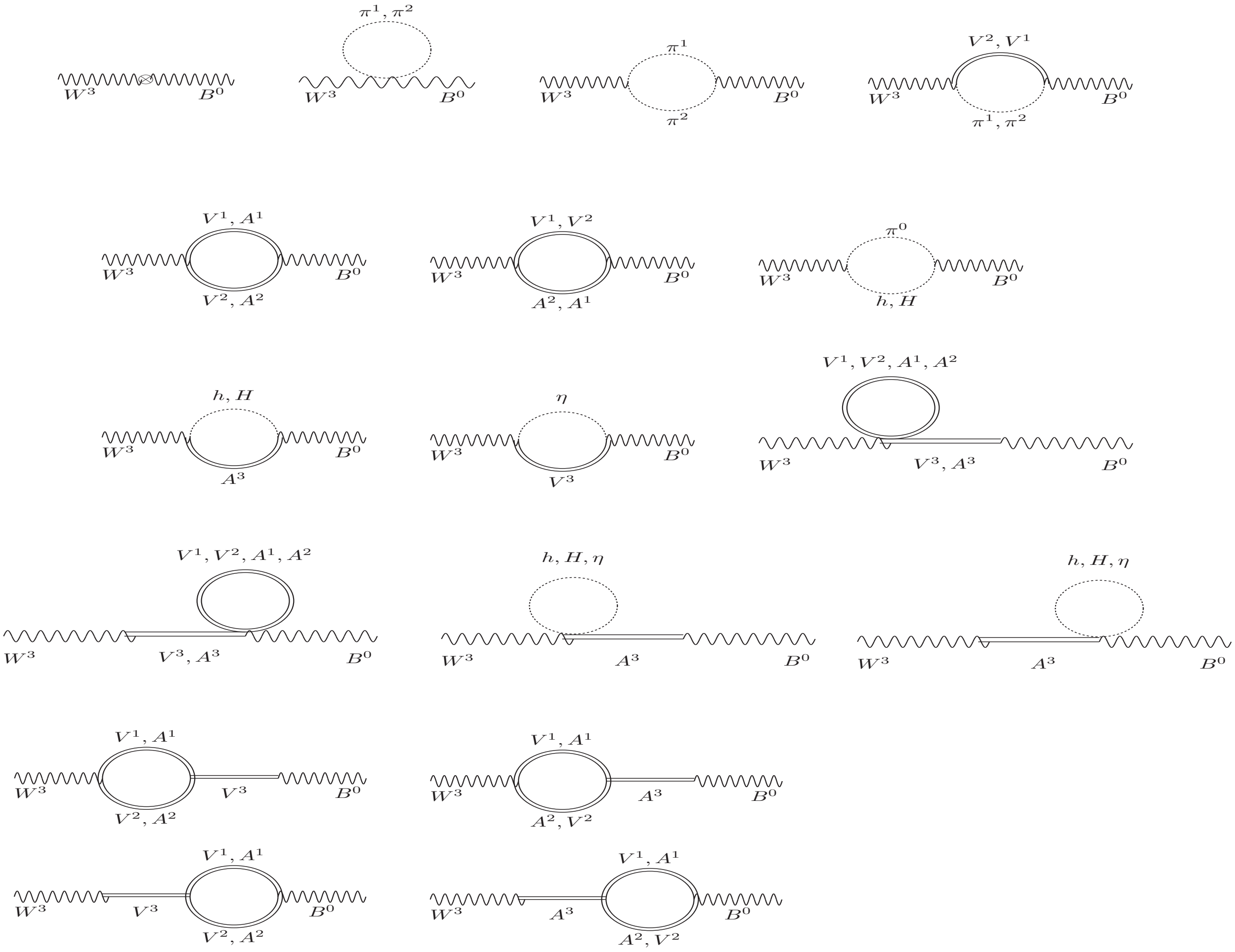

Figure 5. One loop Feynman diagrams contributing to the S parameter.

Corresponding to the Feynman diagrams shown in Figure 5, we decompose the $\widehat{S}$ parameter as:

$$\begin{aligned}
\widehat{S} = {} & \widehat{S}^{(tree)}_{(W^3-B^0)} + \widehat{S}_{(\pi^1\pi^2)} + \widehat{S}_{(\pi^1V^2)} + \widehat{S}_{(\pi^2V^1)} + \widehat{S}_{(V^1V^2)} + \widehat{S}_{(A^1A^2)} \\
& + \widehat{S}_{(V^1A^2)} + \widehat{S}_{(V^2A^1)} + \widehat{S}_{(h\pi^0)} + \widehat{S}_{(H\pi^0)} + \widehat{S}_{(hA^3)} + \widehat{S}_{(HA^3)} + \widehat{S}_{(\eta V^3)} \\
& + \widehat{S}_{(A^2)(W^3-A^3)} + \widehat{S}_{(A^1)(W^3-A^3)} + \widehat{S}_{(A^2)(A^3-B^0)} + \widehat{S}_{(A^1)(A^3-B^0)} \\
& + \widehat{S}_{(V^2)(A^3-B^0)} + \widehat{S}_{(V^1)(A^3-B^0)} + \widehat{S}_{(V^2)(W^3-A^3)} + \widehat{S}_{(V^1)(W^3-A^3)} \\
& + \widehat{S}_{(A^2)(W^3-V^3)} + \widehat{S}_{(A^1)(W^3-V^3)} + \widehat{S}_{(A^2)(V^3-B^0)} + \widehat{S}_{(A^1)(V^3-B^0)} \\
& + \widehat{S}_{(V^2)(V^3-B^0)} + \widehat{S}_{(V^1)(V^3-B^0)} + \widehat{S}_{(V^2)(W^3-V^3)} + \widehat{S}_{(V^1)(W^3-V^3)} \\
& + \widehat{S}^{\left(W^3-V^3\right)}_{(V^1V^2)} + \widehat{S}^{\left(V^3-B^0\right)}_{(V^1V^2)} + \widehat{S}^{\left(W^3-V^3\right)}_{(A^1A^2)} + \widehat{S}^{\left(V^3-B^0\right)}_{(A^1A^2)} \\
& + \widehat{S}^{\left(W^3-A^3\right)}_{(A^1V^2)} + \widehat{S}^{\left(W^3-A^3\right)}_{(V^1A^2)} + \widehat{S}^{\left(A^3-B^0\right)}_{(A^1V^2)} + \widehat{S}^{\left(A^3-B^0\right)}_{(V^1A^2)} \\
& + \widehat{S}_{(h)(W^3-A^3)} + \widehat{S}_{(h)(A^3-B^0)} + \widehat{S}_{(H)(W^3-A^3)} + \widehat{S}_{(H)(A^3-B^0)} \\
& + \widehat{S}_{(\eta)(W^3-A^3)} + \widehat{S}_{(\eta)(A^3-B^0)} + \widehat{S}_{(\pi^1)} + \widehat{S}_{(\pi^2)},
\end{aligned} \tag{B.31}$$

where the different one-loop contributions are:

$$\widehat{S}^{(tree)}_{(W^3-B^0)} = \frac{\pi\alpha_{em}\left(f_V^2 - f_A^2 - c_{WB}\right)}{\sin^2\theta_W}, \tag{B.32}$$

$$\widehat{S}_{(\pi^1\pi^2)} \simeq \frac{\alpha_{em}}{48\pi\sin^2\theta_W}\ln\left(\frac{\Lambda^2}{M_W^2}\right) + \frac{\alpha_{em}f_V g_V}{8\pi v^2\sin^2\theta_W}\Lambda^2, \tag{B.33}$$

$$
\begin{aligned}
\widehat{S}_{(\pi^1 V^2)} = & -\frac{\alpha_{em}}{256\pi v^2 M_V^2 \sin^2\theta_W}\left[6g_V\left(2g_V+\kappa^2 f_V\right)-\frac{16}{3}g_V^2-8\kappa^2 f_V g_V\right]\Lambda^4 \\
& +\frac{\alpha_{em}}{64\pi v^2 \sin^2\theta_W}\Bigg[2\left(f_V-2g_V-\kappa^2 f_V\right)\left(f_V+2g_V+\kappa^2 f_V\right) \\
& +14g_V\left(2g_V+\kappa^2 f_V\right)-16\kappa^2 f_V g_V-\frac{32}{3}g_V^2\Bigg]\Lambda^2 \\
& -\frac{\alpha_{em}}{64\pi v^2 \sin^2\theta_W}\int_0^1 dx\Bigg[2\left(f_V-2g_V-\kappa^2 f_V\right)\left(f_V+2g_V+\kappa^2 f_V\right) \\
& +24g_V\left(2g_V+\kappa^2 f_V\right)x-12\kappa^2 f_V g_V-44g_V^2x^2\Bigg] \\
& \times\left[2M_V^2(1-x)\ln\left(\frac{\Lambda^2+M_V^2(1-x)}{M_V^2(1-x)}\right)-\frac{M_V^2\Lambda^2(1-x)}{\Lambda^2+M_V^2(1-x)}\right] \\
& -\frac{\alpha_{em}}{256\pi v^2 M_V^2 \sin^2\theta_W}\int_0^1 dx\left[6g_V\left(2g_V+\kappa^2 f_V\right)x-24g_V^2x^2-8\kappa^2 f_V g_V\right] \\
& \times\left[6M_V^4(1-x)^2\ln\left(\frac{\Lambda^2+M_V^2(1-x)}{M_V^2(1-x)}\right)-\frac{2M_V^4\Lambda^2(1-x)^2}{\Lambda^2+M_V^2(1-x)}\right] \\
& -\frac{26\alpha_{em}g_V^2M_V^2}{320\pi v^2\sin^2\theta_W}-\frac{3\alpha_{em}g_V^2}{8\pi v^2\sin^2\theta_W}\int_0^1 dx\,x(1-x) \\
& \left\{3M_V^2(1-x)\ln\left(\frac{\Lambda^2+M_V^2(1-x)}{M_V^2(1-x)}\right)+\frac{M_V^4(1-x)^2\left[5M_V^2(1-x)+6\Lambda^2\right]}{2\left[\Lambda^2+M_V^2(1-x)\right]^2}\right\} \\
& -\frac{\alpha_{em}g_V^2}{16\pi v^2 M_V^2\sin^2\theta_W}\int_0^1 dx\,x(1-x)\Bigg\{12M_V^4(1-x)^2\ln\left(\frac{\Lambda^2+M_V^2(1-x)}{M_V^2(1-x)}\right) \\
& -\frac{6M_V^4\Lambda^2(1-x)^2}{\Lambda^2+M_V^2(1-x)}+\frac{M_V^6(1-x)^3\left[M_V^2(1-x)+2\Lambda^2\right]}{\left[M_V^2(1-x)+\Lambda^2\right]^2}\Bigg\},
\end{aligned}
\tag{B.34}
$$

$$
\widehat{S}_{(\pi^2 V^1)} = \widehat{S}_{(\pi^1 V^2)}, \qquad \widehat{S}_{(V^2 A^1)} = \widehat{S}_{(V^1 A^2)}, \tag{B.35}
$$

$$
\begin{aligned}
\widehat{S}_{(V^1 V^2)} = & -\frac{\alpha_{em}\Lambda^2}{24\pi M_V^2\sin^2\theta_W}+\frac{29\alpha_{em}}{96\pi\sin^2\theta_W}\ln\left(\frac{\Lambda^2+M_V^2}{M_V^2}\right)+\frac{9\alpha_{em}}{64\pi\sin^2\theta_W} \\
& -\frac{35\alpha_{em}\Lambda^2}{96\pi\left(\Lambda^2+M_V^2\right)\sin^2\theta_W}-\frac{\alpha_{em}\left(34M_V^2\Lambda^2+27M_V^4\right)}{192\pi\left(\Lambda^2+M_V^2\right)^2\sin^2\theta_W},
\end{aligned}
\tag{B.36}
$$

$$
\begin{aligned}
\widehat{S}_{(A^1 A^2)} = & -\frac{\alpha_{em}\Lambda^2}{24\pi M_A^2\sin^2\theta_W}+\frac{29\alpha_{em}}{96\pi\sin^2\theta_W}\ln\left(\frac{\Lambda^2+M_A^2}{M_A^2}\right)+\frac{9\alpha_{em}}{64\pi\sin^2\theta_W} \\
& -\frac{35\alpha_{em}\Lambda^2}{96\pi\left(\Lambda^2+M_A^2\right)\sin^2\theta_W}-\frac{\alpha_{em}\left(34M_A^2\Lambda^2+27M_A^4\right)}{192\pi\left(\Lambda^2+M_A^2\right)^2\sin^2\theta_W},
\end{aligned}
\tag{B.37}
$$

$$
\begin{aligned}
\widehat{S}_{(V^1A^2)} = {} & \frac{20\,\alpha_{em}\kappa^2\left(M_A^2+M_V^2\right)}{192\pi M_V^2 M_A^2\sin^2\theta_W}\Lambda^2 - \frac{9\,\alpha_{em}\kappa^2}{64\pi\sin^2\theta_W} + \frac{5\,\alpha_{em}\kappa^2\left(M_A^2+M_V^2\right)^2}{256\pi M_V^2 M_A^2\sin^2\theta_W} \\
& - \frac{\alpha_{em}\kappa^2}{8\pi\sin^2\theta_W}\int_0^1 dx\left(x^2-x+\frac{5}{2}\right)\Bigg[\ln\left(\frac{\Lambda^2+M_V^2-\left(M_V^2-M_A^2\right)x}{M_V^2-\left(M_V^2-M_A^2\right)x}\right) \\
& - \frac{\Lambda^2}{\Lambda^2+M_V^2-\left(M_V^2-M_A^2\right)x}\Bigg] - \frac{\alpha_{em}\kappa^2}{64\pi M_V^2 M_A^2\sin^2\theta_W}\int_0^1 dx \\
& \Big[10M_V^2+(26x-3)\,M_A^2-13\left(M_A^2+M_V^2\right)x^2\Big] \\
& \times\Bigg[2\left[M_V^2-\left(M_V^2-M_A^2\right)x\right]\ln\left(\frac{\Lambda^2+\left[M_V^2-\left(M_V^2-M_A^2\right)x\right]}{M_V^2-\left(M_V^2-M_A^2\right)x}\right) \\
& - \frac{\left[M_V^2-\left(M_V^2-M_A^2\right)x\right]\Lambda^2}{\Lambda^2+\left[M_V^2-\left(M_V^2-M_A^2\right)x\right]}\Bigg] \\
& + \frac{9\alpha_{em}\kappa^2}{16\pi\sin^2\theta_W}\int_0^1 dx\,x\,(1-x)\Bigg\{\ln\left(\frac{\Lambda^2+\left[M_V^2-\left(M_V^2-M_A^2\right)x\right]}{\left[M_V^2-\left(M_V^2-M_A^2\right)x\right]}\right) \\
& + \frac{4\left[M_V^2-\left(M_V^2-M_A^2\right)x\right]\Lambda^2+3\left[M_V^2-\left(M_V^2-M_A^2\right)x\right]^2}{2\left(\Lambda^2+M_V^2-\left(M_V^2-M_A^2\right)x\right)^2}\Bigg\} \\
& - \frac{3\alpha_{em}\kappa^2\left(M_A^2+M_V^2\right)}{32\pi M_V^2 M_A^2\sin^2\theta_W}\int_0^1 dx\,x\,(1-x)\Bigg\{3\left[M_V^2-\left(M_V^2-M_A^2\right)x\right] \\
& \times\ln\left(\frac{\Lambda^2+\left[M_V^2-\left(M_V^2-M_A^2\right)x\right]}{\left[M_V^2-\left(M_V^2-M_A^2\right)x\right]}\right) \\
& + \frac{\left[M_V^2-\left(M_V^2-M_A^2\right)x\right]^2\left(5\left[M_V^2-\left(M_V^2-M_A^2\right)x\right]+6\Lambda^2\right)}{2\left(\Lambda^2+\left[M_V^2-\left(M_V^2-M_A^2\right)x\right]\right)^2}\Bigg\},
\end{aligned}
\tag{B.38}
$$

$$
\widehat{S}_{(h\pi^0)} \simeq -\frac{\alpha_{em}\left[(1-\kappa)^{\frac{3}{2}}-2\kappa^{\frac{3}{2}}\right]^2}{384\pi\sin^2\theta_W}\left[\ln\left(\frac{\Lambda^2}{m_h^2}\right)-\frac{1}{6}\right],
\tag{B.39}
$$

$$
\widehat{S}_{(H\pi^0)} \simeq -\frac{\alpha_{em}\left[(1-\kappa)^{\frac{3}{2}}+2\kappa^{\frac{3}{2}}\right]^2}{384\pi\sin^2\theta_W}\left[\ln\left(\frac{\Lambda^2}{m_H^2}\right)-\frac{1}{6}\right],
\tag{B.40}
$$

$$
\widehat{S}_{(hA^3)} = -\frac{\alpha_{em}\kappa\,(1-\kappa)\left(\sqrt{1-\kappa}+2\sqrt{\kappa}\right)^2 M_A^2}{64\pi\left(M_A^2-m_h^2\right)^3\sin^2\theta_W}\left[M_A^4-m_h^4-2m_h^2M_A^2\ln\left(\frac{M_A^2}{m_h^2}\right)\right],
\tag{B.41}
$$

$$
\widehat{S}_{(HA^3)} = -\frac{\alpha_{em}\kappa\,(1-\kappa)\left(\sqrt{1-\kappa}-2\sqrt{\kappa}\right)^2 M_A^2}{64\pi\left(M_A^2-m_H^2\right)^3\sin^2\theta_W}\left[M_A^4-m_H^4-2m_H^2M_A^2\ln\left(\frac{M_A^2}{m_H^2}\right)\right],
\tag{B.42}
$$

$$\widehat{S}_{(\eta V^3)} = -\frac{\alpha_{em}\,(1-\kappa)^2 M_V^2}{32\pi\left(M_V^2 - m_\eta^2\right)^3 \sin^2\theta_W}\left[M_V^4 - m_\eta^4 - 2m_\eta^2 M_A^2 \ln\left(\frac{M_V^2}{m_\eta^2}\right)\right], \tag{B.43}$$

$$\widehat{S}_{(A^2)(W^3-A^3)} = \widehat{S}_{(A^1)(W^3-A^3)} = \widehat{S}_{(A^2)(A^3-B^0)} = \widehat{S}_{(A^1)(A^3-B^0)}, \tag{B.44}$$

$$\widehat{S}_{(A^1)(A^3-B^0)} = \frac{3\alpha_{em}\kappa g_C f_A}{32\pi M_A^2 \sin^2\theta_W}\left\{\frac{\Lambda^4}{2M_A^2} + 3\left[\Lambda^2 - M_A^2 \ln\left(\frac{\Lambda^2 + M_A^2}{M_A^2}\right)\right]\right\}, \tag{B.45}$$

$$\widehat{S}_{(V^2)(W^3-A^3)} = \widehat{S}_{(V^1)(W^3-A^3)} = \widehat{S}_{(V^2)(A^3-B^0)} = \widehat{S}_{(V^1)(A^3-B^0)}, \tag{B.46}$$

$$\widehat{S}_{(V^1)(A^3-B^0)} = \frac{3\alpha_{em}\kappa g_C f_A}{32\pi M_A^2 \sin^2\theta_W}\left\{\frac{\Lambda^4}{2M_V^2} + 3\left[\Lambda^2 - M_V^2 \ln\left(\frac{\Lambda^2 + M_V^2}{M_V^2}\right)\right]\right\}, \tag{B.47}$$

$$\widehat{S}_{(V^2)(W^3-V^3)} = \widehat{S}_{(V^1)(W^3-V^3)} = \widehat{S}_{(V^2)(V^3-B^0)} = \widehat{S}_{(V^1)(V^3-B^0)}, \tag{B.48}$$

$$\widehat{S}_{(V^1)(V^3-B^0)} = -\frac{3\alpha_{em} g_C f_V}{32\pi M_V^2 \sin^2\theta_W}\left\{\frac{\Lambda^4}{2M_V^2} + 3\left[\Lambda^2 - M_V^2 \ln\left(\frac{\Lambda^2 + M_V^2}{M_V^2}\right)\right]\right\}, \tag{B.49}$$

$$\widehat{S}_{(A^2)(W^3-V^3)} = \widehat{S}_{(A^1)(W^3-V^3)} = \widehat{S}_{(A^2)(V^3-B^0)} = \widehat{S}_{(A^1)(V^3-B^0)}, \tag{B.50}$$

$$\widehat{S}_{(A^1)(V^3-B^0)} = -\frac{3\alpha_{em} g_C f_V}{32\pi M_V^2 \sin^2\theta_W}\left\{\frac{\Lambda^4}{2M_A^2} + 3\left[\Lambda^2 - M_A^2 \ln\left(\frac{\Lambda^2 + M_A^2}{M_A^2}\right)\right]\right\}, \tag{B.51}$$

$$\begin{aligned}\widehat{S}^{\left(W^3-V^3\right)}_{(V^1V^2)} = \widehat{S}^{\left(V^3-B^0\right)}_{(V^1V^2)} = \frac{3\alpha_{em} g_C f_V}{64\pi M_V^4 \sin^2\theta_W}\Bigg[&\Lambda^4 + 2M_V^2\Lambda^2 \\ &-6M_V^4 \ln\left(\frac{\Lambda^2 + M_V^2}{M_V^2}\right) + \frac{4M_V^4\Lambda^2}{\Lambda^2 + M_V^2}\Bigg],\end{aligned} \tag{B.52}$$

$$\begin{aligned}\widehat{S}^{\left(W^3-V^3\right)}_{(A^1A^2)} = \widehat{S}^{\left(V^3-B^0\right)}_{(A^1A^2)} = \frac{3\alpha_{em} g_C f_V}{64\pi M_V^2 M_A^2 \sin^2\theta_W}\Bigg[&\Lambda^4 + 2M_A^2\Lambda^2 \\ &-6M_A^4 \ln\left(\frac{\Lambda^2 + M_A^2}{M_A^2}\right) + \frac{4M_A^4\Lambda^2}{\Lambda^2 + M_A^2}\Bigg],\end{aligned} \tag{B.53}$$

$$\widehat{S}^{\left(W^3-A^3\right)}_{(A^1V^2)} = \widehat{S}^{\left(W^3-A^3\right)}_{(V^1A^2)} = \widehat{S}^{\left(A^3-B^0\right)}_{(A^1V^2)} = \widehat{S}^{\left(A^3-B^0\right)}_{(V^1A^2)}, \tag{B.54}$$

$$
\begin{aligned}
\widehat{S}^{(A^3-B^0)}_{(V^1A^2)} = -\frac{3\alpha_{em}\kappa g_C f_A}{128\pi M_A^2\sin^2\theta_W}\Bigg\{ & \frac{M_V^2+M_A^2}{M_V^2 M_A^2}\Lambda^4 + 2\left[6-\frac{\left(M_V^2+M_A^2\right)^2}{M_V^2 M_A^2}\right]\Lambda^2 \\
& -\frac{2M_V^4}{M_V^2-M_A^2}\left(6-\frac{M_V^2+M_A^2}{M_A^2}\right)\ln\left(\frac{\Lambda^2+M_V^2}{M_V^2}\right) \\
& -\frac{2M_A^4}{M_A^2-M_V^2}\left(6-\frac{M_V^2+M_A^2}{M_V^2}\right)\ln\left(\frac{\Lambda^2+M_A^2}{M_A^2}\right)\Bigg\},
\end{aligned}
\tag{B.55}
$$

$$
\widehat{S}_{(h)(W^3-A^3)} = \widehat{S}_{(h)(A^3-B^0)} = -\frac{\alpha_{em} g_C f_A\,(1-5\kappa)}{64\pi M_A^2\sin^2\theta_W}\left[\Lambda^2 - m_h^2\ln\left(\frac{\Lambda^2+m_h^2}{m_h^2}\right)\right], \tag{B.56}
$$

$$
\widehat{S}_{(H)(W^3-A^3)} = \widehat{S}_{(H)(A^3-B^0)} = -\frac{\alpha_{em} g_C f_A\,(1-5\kappa)}{64\pi M_A^2\sin^2\theta_W}\left[\Lambda^2 - m_H^2\ln\left(\frac{\Lambda^2+m_H^2}{m_H^2}\right)\right], \tag{B.57}
$$

$$
\widehat{S}_{(\eta)(W^3-A^3)} = \widehat{S}_{(\eta)(A^3-B^0)} = -\frac{\alpha_{em} g_C f_A\,(1-\kappa)}{32\pi M_A^2\sin^2\theta_W}\left[\Lambda^2 - m_\eta^2\ln\left(\frac{\Lambda^2+m_\eta^2}{m_\eta^2}\right)\right], \tag{B.58}
$$

$$
\widehat{S}_{(\pi^1)} = \widehat{S}_{(\pi^2)} = -\frac{\alpha_{em}\left(2f_V^2 - 2c_{WB} - f_A^2\right)}{8\pi v^2\sin^2\theta_W}\Lambda^2. \tag{B.59}
$$

References

[1] G. Aad *et al.* [The ATLAS Collaboration], "Observation of a new particle in the search for the Standard Model Higgs boson with the ATLAS detector at the LHC," Phys. Lett. **B716**, 1 (2012) [arXiv:hep-ex/1207.7214].

[2] S. Chatrchyan *et al.* [The CMS Collaboration], "Observation of a new boson at a mass of 125 GeV with the CMS experiment at the LHC," , Phys. Lett. **B716**, 30 (2012) [arXiv:hep-ex/1207.7235].

[3] T. Aaltonen *et al.* [CDF and D0 Collaborations], "Evidence for a particle produced in association with weak bosons and decaying to a bottom-antibottom quark pair in Higgs boson searches at the Tevatron," [arXiv:hep-ex/1207.6436].

[4] The CMS Collaboration, "Observation of a new boson with a mass near 125 GeV," CMS-PAS-HIG-12-020.

[5] J. Beringer et al. (Particle Data Group), Phys. Rev. D **86** (2012) 010001.

[6] T. Appelquist and R. Shrock, "Dynamical Symmetry Breaking of Extended Gauge Symmetries," Phys. Rev. Lett. 90, 201801 (2003), [arXiv:hep-ph/0301108].

[7] J. Hirn, A. Martin and V. Sanz, "Benchmarks for new strong interactions at the LHC," JHEP **0805** (2008) 084 [arXiv:hep-ph/0712.3783]. Phys. Rev. D **78** (2008) 075026 [arXiv:hep-ph/0807.2465].

[8] A. Belyaev, R. Foadi, M. T. Frandsen, M. Jarvinen, F. Sannino and A. Pukhov, "Technicolor Walks at the LHC,", Phys. Rev. D **79** (2009) 035006, [arXiv:hep-ph/0809.0793].

[9] C. Quigg and R. Shrock, Phys. Rev. D **79** (2009) 096002 [arXiv:hep-ph/0901.3958].

[10] C. Hill and E. Simmons, Phys. Rep. **381**, 235 (2003) [arXiv:hep-ph/0203079].

[11] J. R. Andersen et al., Eur. Phys. J. Plus 126 (2011) 81 [arXiv:hep-ph/1104.1255].

[12] D. B. Kaplan and H. Georgi, Phys. Lett. B **136** (1984) 183.

[13] M. A. Luty, Phys. Rev. D **41**, 2893 (1990).

[14] R. S. Chivukula and V. Koulovassilopoulos, Phys. Lett. B **309**, 371 (1993) arXiv:hep-ph/9304293].

[15] R. Contino, [arXiv:0908.3578 [hep-ph]].

[16] R. Contino, [arXiv:1005.4269v1 [hep-ph]].

[17] C. Grojean, [arXiv:0910.4976v1 [hep-ph]].

[18] G. F. Giudice, C. Grojean, A. Pomarol and R. Rattazzi, JHEP 0706 (2007) 045 [arXiv:hep-ph/0703164].

[19] R. Barbieri, B. Bellazini, V. S. Rychkov and A. Varagnolo, Phys. Rev. D **76** (2007) 115008 [arXiv:hep-ph/0706.0432].

[20] G. Burdman and L. D. Rold, JHEP **0712** (2007) 086 [arXiv:hep-ph/0710.0623].

[21] P. Lodone, JHEP **0812** (2008) 029 [arXiv:hep-ph/0806.1472].

[22] C. Anastasiou, E. Furlan and J. Santiago, Phys. Rev. D **79** (2009) 075003 [arXiv:hep-ph/0901.2117].

[23] I. Low, R. Rattazzi and A. Vichi, JHEP **1004** (2010) 126 [arXiv:hep-ph/0907.5413]

[24] A. R. Zerwekh, Mod. Phys. Lett. A A25 (2010), 423 [arXiv:hep-ph/0907.4690].

[25] G. Panico, M. Safari and M. Serone, JHEP **1102** (2011) 103 [arXiv:hep-ph/1012.2875]

[26] G. Burdman and C. E. F. Haluch, [arXiv:hep-ph/1109.3914v1].

[27] S. Bar-Shalom, S. Nandi and A. Soni, Phys. Rev. D **84** (2011) 053009 [arXiv:hep-ph/1105.6095].

[28] G. Panico and A. Wulzer, JHEP **1109** (2011) 135 [arXiv:hep-ph/1106.2719].

[29] A. E. Cárcamo Hernández, Claudio. O. Dib, Nicolás Neill H and Alfonso R. Zerwekh, JHEP **1202** (2012) 132 [arXiv:hep-ph/1201.0878].

[30] D. Marzocca, M. Serone and J. Shu, JHEP **1208** (2012) 013 [arXiv:hep-ph/1205.0770].

[31] A. Azatov and J. Galloway, Phys. Rev. D **85** (2012) 055013 [arXiv:hep-ph/1110.5646].

[32] A. Pomarol and F. Riva, JHEP **1208** (2012) 135 [arXiv:hep-ph/1205.6434].

[33] R. Barbieri, D. Buttazzo, F. Sala, D. Straub and A. Tesi, [arXiv:hep-ph/1211.5085].

[34] E. Bertuzzo, T. S. Ray, H. De Sandes and C. A. Savoy, [arXiv:hep-ph/1206.2623].

[35] D. Barducci, A. Belyaev, M.S. Brown, S. De Curtis, S. Moretti, G. M. Pruna, [arXiv:1302.237v1[hep-ph]].

[36] D. Pappadopulo, A. Thamm and R. Torre, arXiv:1303.3062 [hep-ph].

[37] A. Doff, E. G. S. Luna and A. A. Natale, arXiv:1303.3248 [hep-ph].

[38] H. Cai, arXiv:1303.3833 [hep-ph].

[39] R. Contino, M. Ghezzi, C. Grojean, M. Muhlleitner and M. Spira, arXiv:1303.3876 [hep-ph].

[40] C. Delaunay, C. Grojean and G. Perez, arXiv:1303.5701 [hep-ph].

[41] J. Bagger *et al.,* Phys. Rev. D **49** (1994) 1246.

[42] R. Casalbuoni, A. Deandrea, S. De Curtis, D. Dominici, R. Gatto and M. Grazzini, Phys. Rev. D **53** (1996) 5201 [arXiv:hep-ph/9510431].

[43] J. R. Peláez, Phys. Rev. D **55** (1997) 4193 [arXiv:hep-ph/9609427].

[44] R. S. Chivukula, D. A. Dicus and H. J. He, Phys. Lett. B **525** (2002) 175 [arXiv:hep-ph/0111016].

[45] C. Csaki, C. Grojean, H. Murayama, L. Pilo and J. Terning, Phys. Rev. D **69**, 055006 (2004) [arXiv:hep-ph/0305237].

[46] R. Barbieri, G. Isidori, V. S. Rychkov and E. Trincherini, Phys. Rev. D **78** (2008) 036012 [arXiv:0806.1624 [hep-ph]].

[47] O. Cata, G. Isidori and J. F. Kamenik, Nucl. Phys. B **822** (2009) 230 [arXiv:0905.0490[hep-ph]].

[48] R. Barbieri, A. E. Cárcamo Hernández, G. Corcella, R. Torre and E. Trincherini, JHEP **03** (2010) 068 [arXiv:0911.1942[hep-ph]].

[49] A. E. Cárcamo Hernández, [arXiv:1006.1065[hep-ph]], PoS(DIS 2010)185.

[50] A. Orgogozo and S. Rychkov, JHEP **1203** (2012) 046.

[51] A. Pich, I. Rosell and J. J. Sanz-Cillero, JHEP **1208** (2012) 106.

[52] A. Falkowski, C. Grojean, A. Kaminska, S. Pokorski and A. Weiler, JHEP **1111** (2011) 028 [arXiv:hep-ph/1108.1183].

[53] F. Bernardini, F. Coradeschi and D. Dominici [arXiv:hep-ph/1111.4904].

[54] C. Grojean, E. Salvioni, R. Torre, JHEP **07** (2011) 002 [arXiv:hep-ph/1103.2761]].

[55] R. Casalbuoni, S. De Curtis, D. Dominici and R. Gatto, Phys. Lett. B **155** (1985) 95.

[56] R. Casalbuoni, S. De Curtis, D. Dominici and R. Gatto, Nucl. Phys. B **282**, 235 (1987).

[57] R. Casalbuoni, S. De Curtis, D. Dominici, F. Feruglio and R. Gatto, Int. J. Mod. Phys. A **4**, 1065 (1989).

[58] D. Dominici, Riv. Nuovo Cim. **20N11**, 1 (1997) [hep-ph/9711385].

[59] A. R. Zerwekh, Eur. Phys. J. C 46 (2006) 791 [arXiv:hep-ph/0512261].

[60] A. E. Cárcamo Hernández and R. Torre [arXiv:1005.3809[hep-ph]], Nucl. Phys. B **841** (2010) 188.

[61] R. Torre [arXiv:1005.4801[hep-ph]].

[62] A. E. Cárcamo Hernández, [arXiv:1008.1039[hep-ph]], Eur. Phys. J. C **72** (2012) 72:2154.

[63] A. E. Cárcamo Hernández [arXiv:1108.0115[hep-ph]], PhD Thesis.

[64] R. Torre [arXiv:1110.3906[hep-ph]], PhD Thesis.

[65] N. Vignaroli [arXiv:1112.0218[hep-ph]], PhD Thesis.

[66] S. De Curtis, M. Redi and A. Tesi, JHEP **1204** (2012) 042 [arXiv:hep-ph/1110.1613].

[67] M. Redi and A. Tesi, [arXiv:hep-ph/1205.0232].

[68] B. Bellazzini, C. Csaki, J. Hubisz, J. Serra and J. Terning, [arXiv:1205.4032[hep-ph]], to appear in JHEP.

[69] A. Orgogozo and S. Rychkov, arXiv:1211.5543 [hep-ph].

[70] R. Foadi and F. Sannino, arXiv:1207.1541 [hep-ph].

[71] R. Contino, D. Marzocca, D. Pappadopulo and R. Rattazzi, JHEP **1110** (2011) 081 [arXiv:1109.1570[hep-ph]].

[72] D. B. Kaplan, Nucl. Phys. B **365** (1991) 259.

[73] R. Barbieri, G. Isidori and D. Pappadopulo, JHEP **02** (2009) 029 [arXiv:0811.2888 [hep-ph]].

[74] R. S. Chivukula, D. A. Dicus, H. J. He and S. Nandi, Phys. Lett. B **562** (2003) 109 [arXiv:hep-ph/030226].

[75] R. Barbieri, A. Pomarol and R. Rattazzi, Phys. Lett. B **591** (2004) 141 [arXiv:hep-ph/0310285].

[76] Y. Nomura, JHEP **0311** (2003) 050 [arXiv:hep-ph/0309189].

[77] R. Foadi, S. Gopalakrishna and C. Schmidt, JHEP **0403** (2004) 042 [arXiv:hep-ph/0312324].

[78] H. Georgi, Phys. Rev. D **71** (2005) 015016 [arXiv:hep-ph/0408067].

[79] R. S. Chivukula, H. J. He, M. Kurachi, E. H. Simmons and M. Tanabashi, Phys. Rev. D **78**, 095003 (2008), [arXiv:hep-ph/0808.1682].

[80] R. Foadi, M. Järvinen and F. Sannino, Phys. Rev. D **79** (2008) 035010 [arXiv:hep-ph/0811.3719].

[81] M. E. Peskin and T. Takeuchi, Phys. Rev. Lett. 65 (1990) 964; Phys. Rev. D **46**, 381 (1992).

[82] G. Altarelli and R. Barbieri, Phys. Lett. B253 (1991) 161; G. Altarelli, R. Barbieri and F. Caravaglios, Nucl. Phys. B405 (1993) 3.

[83] R. Barbieri, A. Pomarol, R. Ratazzi and A. Strumia, Nucl. Phys. B **703** (2004) 127.

[84] R. Barbieri, "Ten Lectures on Electroweak Interactions", Scuola Normale Superiore, 2007, 81pp, [arXiv:0706.0684[hep-ph]]

[85] M. Bando, T. Kugo and K. Yamawaki, Nucl. Phys. B **259**, 493 (1985).

[86] J. R. Ellis, M. K. Gaillard and D. V. Nanopoulos, Nucl. Phys. B **106**, 292 (1976).

[87] A.I. Vaĭnshteĭn, M.B. Voloshin, V.I. Zakharov and M.A. Shifman, Sov. J. Nucl. Phys. 30 (1979) 711.

[88] L. Okun, *Leptons and Quarks*, Ed. North Holland, Amsterdam, 1982.

[89] M. Gavela, G. Girardi, C. Malleville and P. Sorba, Nucl. Phys. B193 (1981) 257.

[90] J. F. Gunion, H. E. Haber, G. L. Kane and S. Dawson, "The Higgs Hunter's Guide," Front. Phys. **80**, 1 (2000);

[91] M. Spira, Fortsch. Phys. **46**, 203 (1998);

[92] A. Djouadi, Phys. Rept. **457**, 1 (2008).

[93] W. J. Marciano, C. Zhang and S. Willenbrock, Phys. Rev. D **85**, 013002 (2012) [arXiv:1109.5304 [hep-ph]].

[94] Lei. Wang and Xiao-Fang Han, Phys. Rev. D **86**, 095007 (2012), [arXiv:hep-ph/1206.1673].

[95] Chen Chian-Shu, private communication.

[96] CERN Report No. ATLAS-CONF-2012-170, 2012 (unpublished).

[97] CERN Report No. CMS-PAS-HIG-12-045, 2012 (unpublished).

[98] CMS Higgs TWiki, https://twiki.cern.ch/twiki/bin/view/CMSPublic/Hig12045TWiki.

[99] M. Baak *et al.*, “Updated Status of the Global Electroweak Fit and Constraints on New Physics,” Eur. Phys. J. C72 (2012) 2003, [arXiv:1107.0975[hep-ph]]

[100] A. Pich, I. Rosell and J. Sanz-Cirello, [arXiv:hep-ph/1212.6769].